IEEE Access
Multidisciplinary | Rapid Review | Open Access Journal

Received October 22, 2016, accepted November 12, 2016, date of publication November 15, 2016, date of current version January 27, 2017.

Digital Object Identifier 10.1109/ACCESS.2016.2628776

Performance of Cognitive Selective-Repeat Hybrid Automatic Repeat Request

ATEEQ UR REHMAN, VARGHESE ANTONY THOMAS, LIE-LIANG YANG, (Fellow, IEEE), AND LAJOS HANZO, (Fellow, IEEE)

School of Electronics and Computer Science, University of Southampton, Southampton, SO17 1BJ, U.K.

Corresponding author: L. Hanzo (lh@ecs.soton.ac.uk)

The work of A. U. Rehman was supported by the Abdul Wali Khan University, Mardan, Pakistan, through the faculty development Program. This work was supported in part by the EPSRC under Project EP/Noo4558/1 and Project EP/L018659/1, in part by the European Research Council's Advanced Fellow Grant under the Beam-Me-Up Project, and in part by the Royal Society's Wolfson Research Merit Award. The research data for this paper is available at http://dx.doi.org/10.5258/SOTON/403147.

ABSTRACT In this paper, a novel transmission protocol is proposed based on the classical selective-repeat hybrid automatic repeat to access a primary user (PU) channel, which is referred to as the CSR-HARQ. We assume that the PU transmits information based on time-slots (TSs). During a TS, the cognitive radio transmitter first senses the PU channel. Once a free TS is found, it transmits a number of packets to the CU receiver based on the principles of the SR-HARQ. In this paper, we analyze the throughput, average packet delay, and end-to-end packets delay of the CSR-HARQ. We proposed a pair of analytical approaches. The first one is probability based, while the second one relies on the classic discrete time markov chain principles. Finally, we study the throughput, average packet delay, and the end-to-end packet delay of the CSR-HARQ both by simulations and by evaluating our formulas. The simulation-based studies agree well with the analytical results. The performance of the CSR-HARQ systems is significantly impacted by the activity of the PU channel and by the reliability of the spectrum sensing.

INDEX TERMS Cognitive radio, primary users, selective-repeat, HARQ, DTMC, spectrum sensing transmission reliability, throughput, delay, PMF.

LIST OF ACRONYMS

ACK	Positive Acknowledgement
ARQ	Automatic Repeat ReQuest
Busy	TS occupied by the PU
CGBN	Cognitive Go-Back-N
CR	Cognitive Radio
CSR	Cognitive Selective-Repeat
CSW	Cognitive Stop and Wait
CU	Cognitive User
DTMC	Discrete Time Markov Chain
DSA	Dynamic Spectrum Access
e	Erroneous Packet
FEC	Forward Error Correction
Free	TS free from PU
GBN	Go-Back-N
GF	Galois Field
HARQ	Hybrid Automatic Repeat ReQuest
NACK	Negative Acknowledgement
OFF	Markov chain in OFF state
ON	Markov chain in ON state
PEP	Packet Error Probability
PMF	Probability Mass Function
PPS	Packet Per Second
PPTS	Packet Per Time-slot
PPT_p	Packet Per T_p
PR	Primary Radio
PU	Primary User
RS	Reed-Solomon
RTT	Round-Trip Time
SR	Selective-Repeat
SW	Stop-and-Wait
TS	Time-slot

LIST OF SYMBOLS

α	Transition probability from 'ON' to 'OFF' state
b	Represents a busy TS
β	Transition probability from 'OFF' to 'ON' state
B	Final successful reception of a packet
c	Represents transition from state S_i to S_j after a certain delay
$\boldsymbol{d}$	Vector for storing the end-to-end delay of packets

E	Average
f	Represents an erroneous transmission
G	Number of retransmissions of a packet
k	Duration for sensing the TS
K_d	Information Bits
$l_{i,j}$	Number of new packets transmitted in state S_i are correctly received in state S_j
M_c	Total number of packets
M_T	Maximum delay
N	Number of packets in a TS
N_d	Coded symbols
N_s	Number of successfully received packets
N_t	Number of TSs considered in simulation
L_i	Number of new packets transmitted from state S_i
$\boldsymbol{P}$	Transition matrix
$\boldsymbol{P}_d$	PMF of end-to-end delay obtained through simulation
P_e	Packet error probability
$P_{i,j}$	$\{i,j\}$th element of the transition matrix
P_{MF}	Probability distribution of end-to-end packet delay
P_{off}	Probability of the PU's channel being free from the PUs
P_{on}	Probability of the PU's channel being occupied by the PUs
π_i	ith element of steady-state vector
R_B	Receiver buffer
R_s	Throughput
R'_s	Normalized throughput
R'_S	Simulation throughput
$\mathbb{S}$	Sample set
S_i	Represents state i
$\mathbb{S}_N$	Subset of $\mathbb{S}$
$\mathbb{S}_i$	Subset of $\mathbb{S}_N$, which contains states associated with new packets
s	Final successful transmission
$[\,]^T$	Transpose of matrix
T	Duration of the TS
T_i	ith TS
T_B	Transmitter buffer
T_d	Data transmission epoch
T_D	Total average packet delay obtained from theory
T_{DP}	Delay due to busy channels
T_{DS}	Total average packet delay obtained using simulation
T_p	Duration of packet transmission
T_s	Sensing epoch
τ	Average end-to-end packet delay obtained through theory
τ_s	Average end-to-end packet delay obtained by simulation
$\mathbf{1}$	Column vector containing 1

I. INTRODUCTION

The 21st century has seen a shortage of spectrum bands for innovative new wireless applications. Recent studies have shown that the spectrum scarcity is more a consequence of the sub optimum static spectrum allocation, rather than because of the physical shortfall of electromagnetic spectrum [1]–[6]. Under the static allocation policy, the spectral bands are solely allocated to the primary users (PUs) for exclusive use, having several bands under-utilized in both the temporal as well as the spatial domain [1].

Since the permanently allocated spectrum is often utilized inefficiently, dynamic spectrum access may be preferred [7]–[10]. To elaborate a little further, this solution allows cognitive users (CUs) to opportunistically exploit the unoccupied spectrum, while ensuring that the communication of PUs remains unaffected [11], [12]. If the channel is found to be occupied by the PUs, then the CU waits for it to become free [12]. Moreover, the CUs have to curtail their transmissions as soon as the PUs become active. The CR philosophy was introduced by Mitola and Maguire [11] and it has been subsequently incorporated in various wireless standards, such as the wireless regional area networks (WRANs) specified by IEEE 802.22 standard, IEEE 1900, 802.11y, 802.22 [13].

In this context, we propose the Cognitive Selective Repeat HARQ (CSR-HARQ) scheme for a spectrum overlay environment [8], [10], [29], [30], which relies on the CU's ability to sense the activity of PUs over the channel and to access it for its own transmission, when the channel is deemed to be free at the time of the CU's request to transmit, as shown in Fig. 1. Similar to our previous studies [31]–[34], the activity of PU is modelled using a two-state Discrete Time Markov chain (DTMC), having 'ON' and 'OFF' states [35], [36]. The CU is only allowed to communicate, when the PU is in the 'OFF' state, which implies that the PU is silent. Otherwise, the CU continues sensing the channel until it is found to be in the 'OFF' state. Furthermore, the temporal partitioning of the channel into T seconds long time-slots (TS) is relied upon, where the PUs employ time division multiplexing. Furthermore, for the CR system, each free TS is further partitioned into sensing epochs of T_s seconds followed by a transmission epoch of T_d seconds as shown in Fig. 1 [35], [37]. Specifically, the sensing duration is T_s, while the remaining $T_d = T - T_s$ duration is invoked for data transmission during the 'OFF' state. Spectrum sensing has been widely studied. In [38] Akyildiz *et al.* provided a survey related to spectrum management and CR architectures. Yucek and Arslan [39] proposed a multi-dimensional sensing technique for detecting the PU's transmission. The state-of-the-art of spectrum sensing and recent advances were reviewed by Axell *et al.* [40]. Moreover, an optimal sensing and TS duration have been determined by Liang *et al.* in [41] and Tang *et al.* [42] for the sake of maximizing throughput of the CUs. As further development, Stotas and Nallanathan [37] provided the trade-off between the sensing duration and throughput, which has been optimized by proposing a hybrid spectrum sensing and data transmission technique. Liang *et al.* [43] proposed a cooperative CR system in which the PUs trade with CUs and allocate the free TSs on the basis of reducing the transmission power and maximizing the transmission rate.

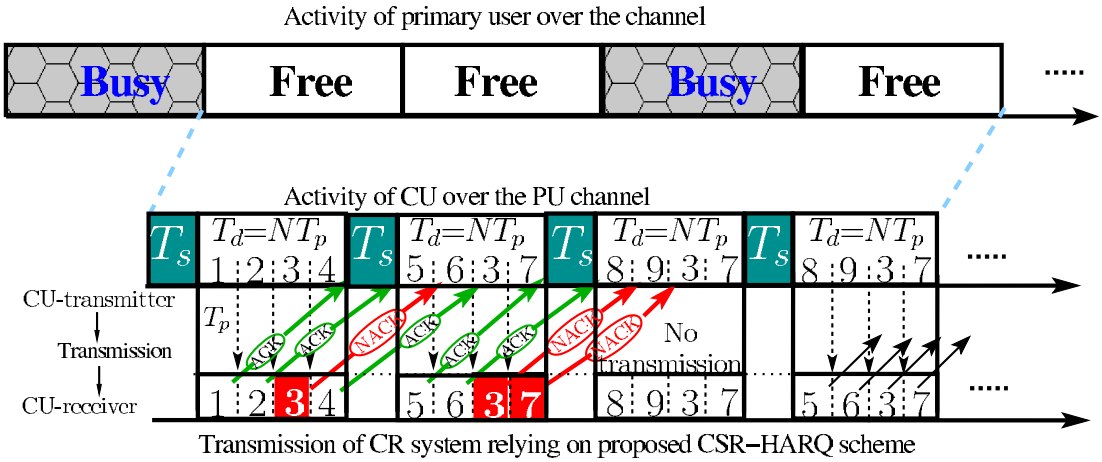

FIGURE 1. Transmission flow of the proposed CSR-HARQ in the presence of both free and busy TSs. Each TS has the duration of $T = T_s + T_d$ seconds and in each free TS, $N = 4$ packets are transmitted where T_p is the duration required for the transmission of a packet.

Naturally, CR system suffer both from interference, noise, fading and other impairments [44]–[46]. To achieve both a high integrity and a high throughput, robust error correction techniques have been proposed for both the physical and data link layer [47], [48]. For example, powerful anti-jamming coding by Yue *et al.* in [49], [50] for CR systems. As a further advancement, Liu *et al.* [51] proposed a network-coding technique for classic ARQ protocols. Zhong and Hanzo [52] introduced HARQ-based superposition coding for improving both the cell-edge coverage and the energy efficiency. The end-to-end delay is minimized by reducing the number of retransmissions using HARQ [53]. Furthermore, Makki *et al.* [54] used HARQ protocols and investigated both the throughput and outage probability, while in [55] Makki *et al.* invoked block coding for improving the throughput. Ngo and Hanzo [56] studied the state-of-the-art of HARQ scheme in cooperative wireless scenarios. As a further development, Liang *et al.* [57] conceived an adaptive dynamic network coding technique for cooperative communication between the PUs and CUs, whilst relying on powerful turbo trellis coded modulation (TTCM). In a nutshell, in Fig. 2, we have presented the evolution of HARQ scheme in CR scenarios at glance.

Our proposed CSR-HARQ transmission scheme intrinsically incorporates the SR-HARQ protocol into the CR system. We advocate the SR-HARQ scheme over other ARQ schemes, as benefit of its improved throughput and delay. This is achieved at the cost of resequencing buffer for queuing the out-of-order error-free packets. Explicitly, it is depicted in Fig. 1 that the channel is initially sensed by the CU transmitter and provided that it is deemed to be free from PUs, then the CU transmits its packets relying on SR-HARQ protocol. The CU receiver receives packets in a chronological order and transmits an acknowledgement to the CU transmitter after each packet. A new packet is transmitted by the CU transmitter after receiving a positive feedback (ACK). By contrast, for a negative feedback (NACK), the related packet is retransmitted, provided that the channel is deemed to be free.

The performance of the classical Selective-Repeat (SR) protocol has been lavishly published in [58]–[61]. In particular, Kim and Krunz [58] as well as Ausavapattanakun and Nosratinia [59] investigated the throughput as well as the delay of the SR-HARQ technique using a Markov chain. Moreover, Badia *et al.* [60] analysed the delay as well as throughput of the SR technique using the moment-generating function and quantified the detrimental effects of practical imperfect feedbacks modelled by a hidden Markov model. The total delay of transmission, queuing and resequencing was also quantified for the classical SR-ARQ regime by Badia [61]. Chen *et al.* [62] discussed the challenges of amalgamating HARQ with turbo codes for reducing the complexity. As a further advance, a distributed multiple component turbo code (MCTC) was also designed [63] for cooperative HARQ, for the sake of reducing the decoding complexity compared to the classic twin-component turbo parallel code. Moreover, in [64], the so-called absorbing Markov chain theory was conceived by Chiti *et al.* for modelling the SR-ARQ for investigating its resequencing delay. By contrast, the probability distribution of the packet delay was analysed by Dong *et al.* [65], [66].

Given the stochastic nature of the PUs ON/OFF pattern, its theoretical analysis in an ARQ-aided CR environment is a challenge. Hence, there is a paucity of contributions on this subject [19], [44]–[46], [67]–[69], because, these have left the theoretical throughput and delay analysis of the ARQ protocols open. Specifically, Ao and Chen [67] as well as Touati *et al.* [68] analysed the performance of their relay-aided ARQ protocol in CR environments. By contrast, the throughput of a SR-ARQ protocol aided CR-based multi-hop relaying system was studied by Jeon and Cho [19]. Park *et al.* [69] quantified the throughput gain attained in the absence of inference imposed on the PUs transmission.

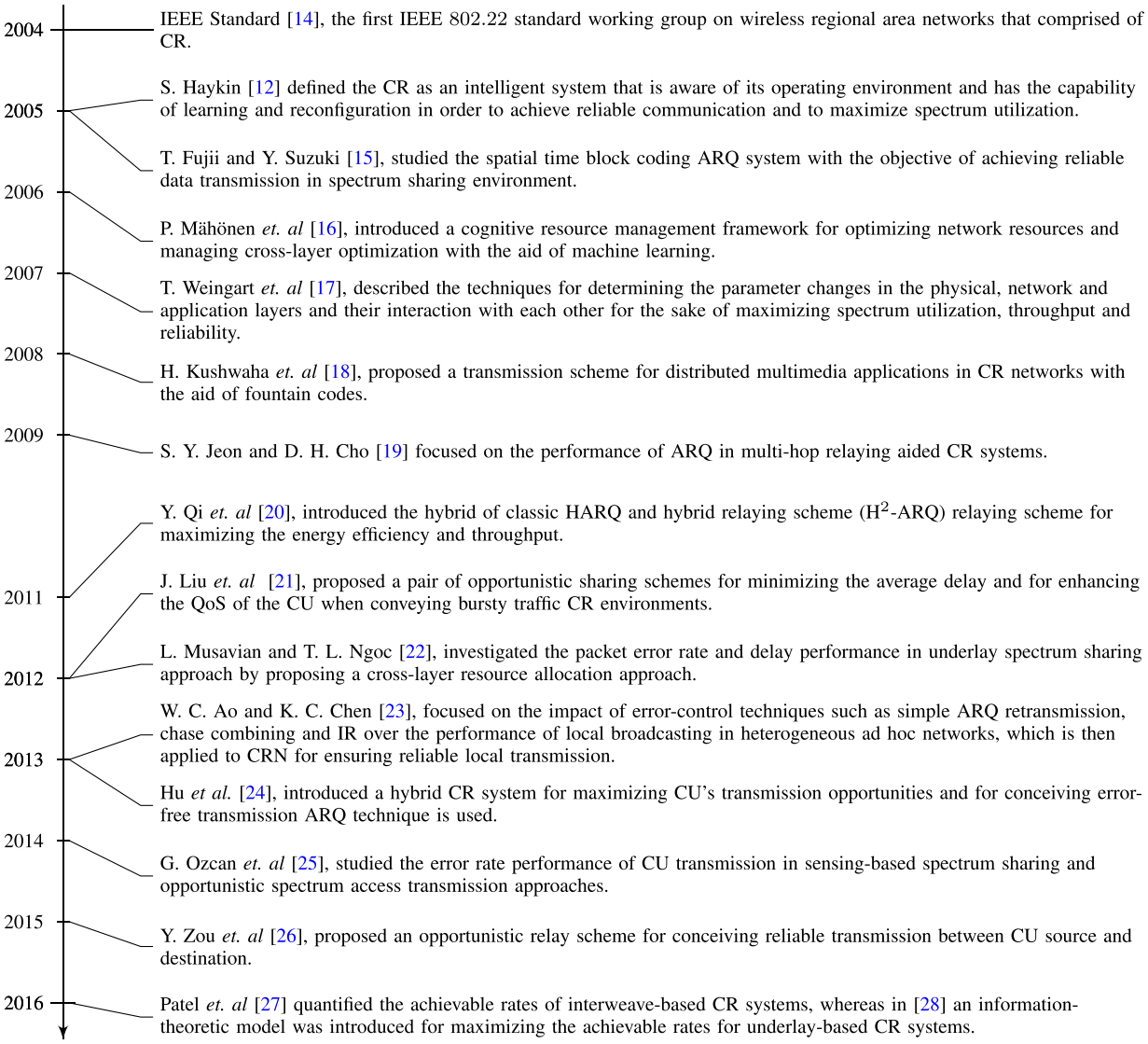

FIGURE 2. **Timeline of cognitive radio research in the context of HARQ.**

Then Roshid *et al.* [70] reviewed various cooperative sensing and transmission techniques between the CUs and PUs for the sake of improving the throughput, while avoiding collisions between the PUs and CUs. Finally, [44]–[46] offered a detailed survey of the sophisticated CR systems.

A. CONTRIBUTION AND PAPER STRUCTURE

This paper is inspired by our own prior contributions [31]–[34], in which we studied the performance of the Cognitive Stop-and-Wait HARQ (CSW-HARQ) and Cognitive Go-Back-N HARQ (CGBN-HARQ), when both reliable and realistic imperfect sensing are assumed. Specifically, in [31] and [32], we studied the performance of the CSW-HARQ protocol, which enables the CU transmitter to transmit a single packet in each free TS and waits for its feedback assumed to be received within the same TS. After the reception of feedback, the transmitter (re)transmits a packet, if the following TS is found to be free. By contrast, in [33] and [34], the CU transmitter is programmed to continuously transmit N packets one after another to the CU receiver, without waiting for the related feedback. After the reception of each packet, the CU performs error correction/decoding and then generates its feedback to be sent back to the transmitter. If an ACK is received, the transmitter transmits a new packet, provided that the TS is found free. Otherwise, if a NACK is received, the transmitter transmits the erroneous packet as well as the subsequent packets (transmitted after the erroneous packet), regardless whether they are error-free or not. The unnecessary retransmission of the subsequent packets causes delay, since the packets have to wait for the correct reception of the previous packets. Hence, to avoid unnecessary transmissions, in this paper, a buffer of size N is provided at the receiver, which results in a more complex CU receiver but improves both the throughput and the delay.

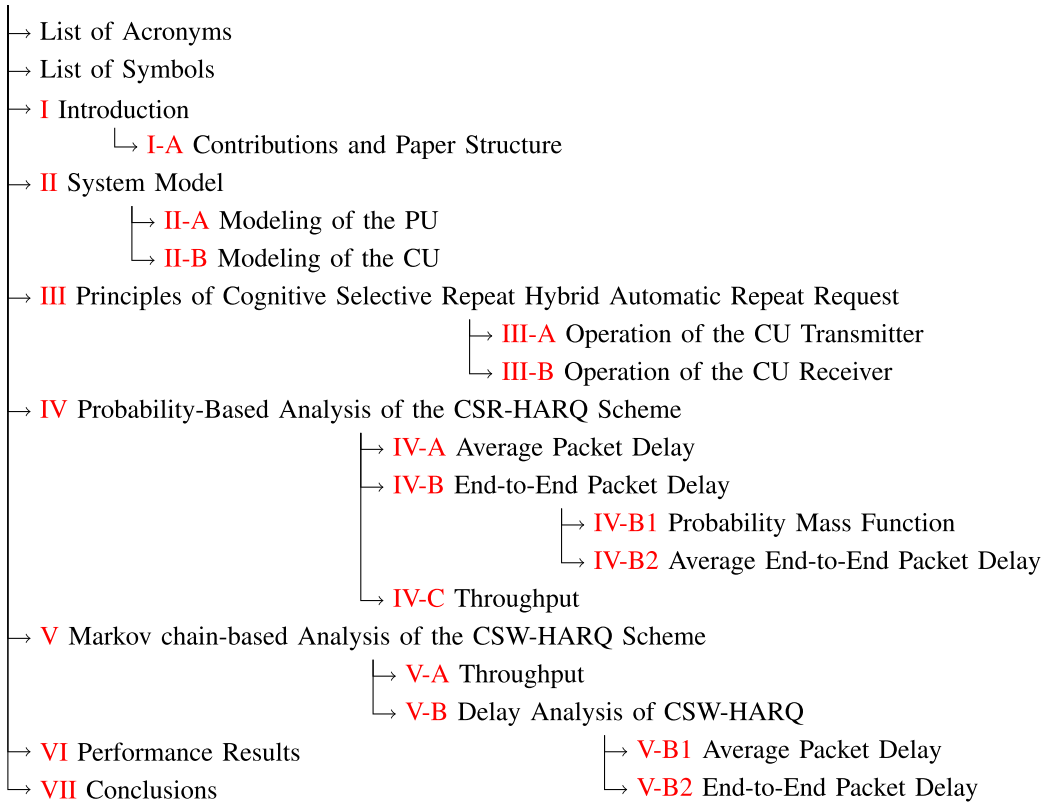

FIGURE 3. The structure of this paper.

Against the above background, the contributions of this manuscript may be summarised as follows:

(a) We propose a novel CR protocol, namely CSR-HARQ, for attaining reliable communication. The proposed scheme is based on the classic SR-HARQ scheme. The CU transmitter in our protocol senses the channel before using it and it can always receive feedback, regardless of its specific activity (waiting, sensing or transmitting). However, fulfilling this requirement demanded a significant reformulation of the SR-HARQ transmission principles.

(b) Firstly, a probability-based technique has been used to model and to theoretically analyse the proposed scheme. We derived closed-form expressions for the CR system's average packet delay, throughput as well as end-to-end packet delay. Expressions for the probability distribution of the end-to-end packet delay as well as for the average end-to-end packet delay have also been derived.

(c) Secondly, the proposed scheme has been also modelled and to theoretically analysed by using a DTMC approach. Relying on this approach we derived closed-form expressions for generating DTMC state index, the total number of states, the throughput of the CR system, the average packet delay as well as the end-to-end packet delay. Expressions for the probability distribution of the end-to-end packet delay as well as for the average end-to-end packet delay have also been derived.

(d) Ultimately, we provide a simulation-based validation of both the theoretical probability-based methodology and of the Markov chain based methodology.

The outline of this paper is as follows. In Section II, we model the activities of PU and CU. Section III offers a discussion of the proposed CSR-HARQ transmission scheme. The operation of the CU transmitter is discussed in Section III-A, while that of the CU receiver is detailed in Section III-B. In Section IV we model the proposed CSR-HARQ scheme using a probability-based approach while in Section V model it using a Markov chain-based approach. Both the delay and the throughput of the CSR-HARQ are analysed in both sections. Subsequently, we present the simulation-based system performance in Section VI. Finally, we offer our conclusions in Section VII.

II. SYSTEM MODEL

A. MODELLING OF THE PU

Let us assume that the wireless channel is exclusively allocated to the PUs, using the classic TDMA technique, where each TS has a duration of T seconds. Each TS has the same probability of activation, which is also independent from the other TSs. The utilization of the channel by the PUs may be modelled using the DTMC presented in Fig. 4, which has the 'ON' and 'OFF' states. We assume that the probability of the

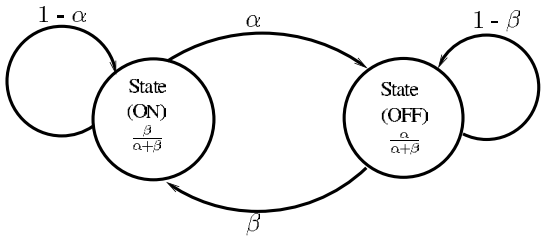

FIGURE 4. Discrete-time two-state Markov chain modelling the 'ON' 'OFF' process of PU system.

channel making a transition from 'ON' to 'OFF' is α, while the probability of the reverse transition is β. Moreover, we assume that the channel obeys the probabilities P_{on} and P_{off} of being in the 'ON' and 'OFF' states, respectively, where we have $P_{off} = 1 - P_{on}$. By definition, the Markov chain is said to be steady, when we have [71],

$$P_{on}\alpha = P_{off}\beta, \tag{1}$$

yielding:

$$P_{on} = \frac{\beta}{\alpha + \beta}, \quad P_{off} = \frac{\alpha}{\alpha + \beta}. \tag{2}$$

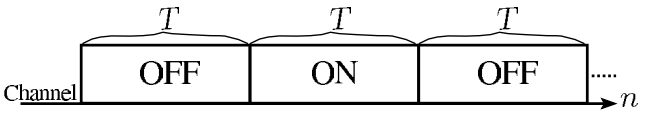

(a) Pattern of channel usage by PR

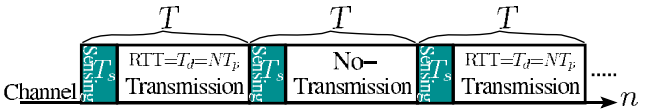

(b) Pattern of channel usage by CR

FIGURE 5. Time-slot structure of PU and CU systems, where a CU TS consists of a sensing duration of T_s and a transmission duration of $T_d = T - T_s$, when given the total duration T of a time-slot. (a) Pattern of channel usage by PR. (b) Pattern of channel usage by CR.

The employment of TDMA ensures that PU's transmission duration is always quantized to an integer multiple of the TS duration T, as shown in Fig. 5(a). For example, the duration of the PU transmission may be equal $2T$ or $3T$ seconds but never to $2.5T$ seconds. Additionally, time synchronization of the TDMA system ensures that the start and end of the PU transmission corresponds to the start and end of the TSs, respectively. It becomes clear from the above discussion that, in the PU's 'OFF' state, the CU may acquire the channel for its own transmission without interfering with the transmissions of the PUs. Having modelled the activity pattern of the PUs, we now model that of the CU in the next section.

B. MODELLING OF THE CU

As discussed in the previous section, we assumed that the CU may acquire the channel for its own transmission by following the spectrum overlay technique [8], [10], [29], which constrains it to use the channel only when it is free from PU's transmissions. Just like the PU, the CU too acquires the channel for a duration, which equals an integer multiple of the TSs. However, unlike the PU, the CU does not utilize the entire TS duration for data transmission. Instead, it divides each TS into two phases, namely, the sensing phase of duration T_s seconds and the transmission phase of duration $T_d = T - T_s$ seconds as shown in Fig. 5(b). We assume that CU transmits N packets in the transmission duration of T_d. Thus, if T_p seconds are needed for the transmission of a single packet, we can state that $T_d = NT_p$. For ease of analysis, we assume that the sensing duration too equals an integer multiple of T_p, i.e. $T_s = kT_p$ seconds. An underlying assumption of our analysis is that the CU is capable of ideally sensing the activity of the PUs without miss-detection or false-alarm. Here, miss-detection refers to the CU falsely concluding that the channel is free, while false-alarm refers to the CU falsely detecting the channel to be busy. In the next section, we discuss the proposed CSR-HARQ scheme employed by the CU for transmitting its data during the free TSs.

III. PRINCIPLES OF COGNITIVE SELECTIVE REPEAT HYBRID AUTOMATIC REPEAT REQUEST

The proposed CSR-HARQ scheme relies on Reed-Solomon (RS) decoder at the receiver for detecting as well as correcting the errors imposed by the channel, which is denoted as RS(N_d, K_d) [47], where K_d and N_d denote the number of original information and coded symbols, respectively. We assume that each N_d − symbol packet is protected by a single RS codeword. The error detection capability of the RS code is assumed to be ideal, while it is capable of correcting upto $t = \frac{N_d - K_d}{2}$ erroneous symbols. The packet is said to be erroneous when the channel inflicts more than t errors.

The round-trip-time (RTT) of a packet is equal to T_d seconds, which is the time between its transmission and the reception of its feedback flag. Hence, during the RTT, the CU can also transmit upto $(N - 1)$ subsequent packets before receiving its feedback.

Given these assumptions, the operation of our CSR-HARQ scheme is shown in Fig. 6. Specifically, when a free TS is found, the CU transmitter sends a sequence of N packets to the receiver, where a feedback signal is generated for each of the packets for notifying the transmitter whether the packet is received error-free or in error. The operation of CSR-HARQ is formally stated in Algorithm 1 as detailed in sections III-A and III-B.

A. OPERATION OF CU TRANSMITTER

In the classic SR-HARQ scheme, the transmitter only has to retransmit those specific packets for which we receive NACK signals. Hence, upon receiving a positive ACK flag for a previous packet, a new packet is transmitted. By contrast, observe our proposed CSR-HARQ scheme both in Fig. 6 and in Algorithm 1 that the CU transmitter first senses the channel

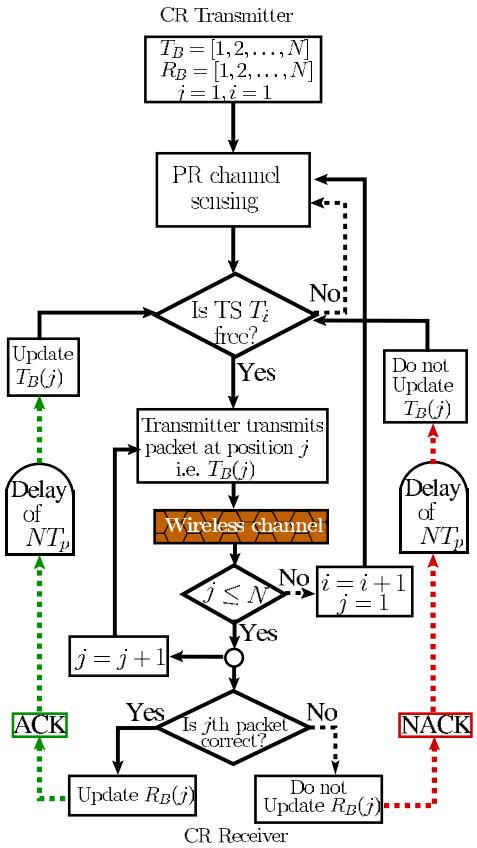

FIGURE 6. Flow chart showing the operations of the proposed CSR-HARQ scheme, where T_B and R_B represent the transmitter and receiver buffer, respectively. The transmitter receives the feedback of each packet after NT_p seconds of its transmission.

for T_s seconds and then transmits or retransmits its packets during the ensuing T_d seconds, if the PU's channel is deemed to be free, as presented on line 6 and 24 of Algorithm 1. However, if the PU's channel is found to be busy in a TS, then the CU has to wait until the next TS, as illustrated on line 32 and 26 of Algorithm 1. In the proposed CSR-HARQ scheme, we have assumed that the CU always has packets in its buffer to transmit, that all packets are of the same length, and each of the packet is transmitted in T_p seconds. As mentioned in Section III, the ACK/NACK feedback of each transmitted packet is assumed to be received after the RTT of T_d seconds without error. Furthermore, as in the classical SR-ARQ, we assume that the CU transmitter has a buffer of size N [47], [71], where packets are entered and transmitted in a first-in-first-out (FIFO) fashion, with their copies being kept in the transmitter's buffer until they are positively acknowledged. If this is the case, then the buffer is updated, as shown on line 18 of Algorithm 1. Moreover, we also assumed that the CU transmitter may receive feedback both during free and busy TSs. This assumption may be justified, since the feedback flag is a single-bit message [72], [73]. Hence, the CU transmitter does not have to wait for a free TS to receive feedback concerning the packets transmitted in the previous free TS.

Algorithm 1 CSR-HARQ

1: **Initialization**: M_c = number of packets, $T_d = N$, $T_s = k$, $i = 1$, TS= 1, $T_B = [1, 2, \ldots, N]$, $R_B = [1, 2, \ldots, N]$.
2: **Input:** N, k, packets.
3: **while** $i \leq M_c$ **do**
4: CU transmitter senses a TS.
5: **if** TS is free **then**
6: Transmitter transmits N packets from the buffer T_B.
7: $j = 1$, $a = 0$, $b = 0$, TS=TS+1.
8: **while** $j \leq N$ **do** ▷ Check each received packet.
9: **if** Packet at position $R_B(j)$ is correctly received **then**
10: Transmit ACK signal for the respective packet and update receiver's buffer R_B.
11: $R_B(j) = R_B(j) + N - a$.
12: **else**
13: Receiver transmits NACK for the packet at position $R_B(j)$ and $R_B(j)$ remains unchanged.
14: $a = a + 1$.
15: **end if**
16: **if** ACK is received for a packet at position $T_B(j)$ **then**
17: Transmitter updates buffer at position $T_B(j)$.
18: $T_B(j) = T_B(j) + N - b$.
19: **else** NACK is received for a packet at position $T_B(j)$, then
20: Transmitter's buffer $T_B(j)$ is not updated.
21: $b = b + 1$.
22: **end if**
23: **if** TS is free & feedback is received during T_d period **then**
24: A new or old packet at position $T_B(j)$ is transmitted.
25: **else** TS is busy || feedback is received during T_s period
26: No transmission and wait.
27: **end if**
28: $j = j + 1$.
29: **end while**
30: $i = \max(R_B)$ ▷ how many packets are correctly received
31: **else**
32: transmitter waits for the next TS.
33: TS=TS+1.
34: **end if**
35: **end while**

For instance, consider the ideal scenario of Fig. 7, where the CU transmits N packets from the transmitter's buffer within the free TS T_1. In Fig. 7, all packets transmitted in TS T_1 are correctly received and, correspondingly, positive

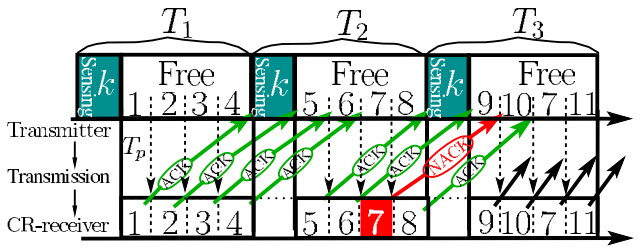

FIGURE 7. Transmission flow of error-free and erroneous packets based on the principle of CSR-HARQ scheme for $N = 4T_p$ and $T_s = k = 1T_p$.

ACKs are sent back by the CU receiver. Upon receiving an ACK, the transmitter removes the corresponding copy of the packet from the buffer and fills the vacant space with a new packet. This process repeats, provided that the following TS is sensed free and that the transmitted packets are positively acknowledged. However, if a NACK is received for a packet, say at the *j*th position, as shown in Fig. 7, then the transmitter's buffer is not updated and the corresponding packet is retransmitted without influencing the other packets.

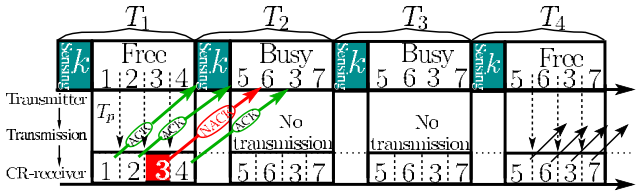

FIGURE 8. Transmission flow of error-free and erroneous packets in the presence of busy TS for $N = 4T_p$ and $T_s = k = 1T_p$.

In the case that there are busy TSs, as shown in Fig. 8, where a free TS is followed by a busy TS, the CSR-HARQ acts as follows. During the free TS T_1, the transmitter transmits $N = 4$ packets. It can be seen that packets 1, 2 and 4 are successfully delivered, while packet 3 is in error. Consequently, the transmitter's buffers $T_B(j)$ are updated at positions $j = 1, 2$ and 4 by new packets, while $T_B(3)$ remains unchanged. Furthermore, as shown in Fig. 8, T_2 and T_3 are busy, hence the CU is not allowed to transmit. Therefore, it waits until the next TS of T_4. In the TS T_4, the four packets having indices 5, 6, 3 and 7 are transmitted.

B. THE OPERATION OF CU RECEIVER

Similar to the classic SR-HARQ scheme [47], [71], [74], the CSR-HARQ receiver has a buffer of size N for storing the indices of the packets that the receiver is expecting to receive. Upon receiving a packet, the CU receiver checks whether the index of this packet matches the index in the receiver's buffer. If so, then the CU receiver invokes the RS decoding and generates the corresponding ACK or NACK depending on whether the received packet is error-free or in error. Furthermore, the CU's receiver buffer is updated, if the packet is error-free. In Algorithm 1, these operations are presented on lines 9 to 15. Additionally, the operations of the CU receiver may be interpreted using the examples depicted in Figs. 7 and 8, where we can see that the CU receiver only accepts those packets having the same index as those expected by the CU receiver. Note that although the receiver may receive the packets, out of ordered it delivers the packets to the higher ISO layers in the correct order [47], [71]–[73].

IV. PROBABILITY-BASED ANALYSIS OF THE CSR-HARQ SCHEME

We employ three metrics for studying the performance of the proposed CSR-HARQ scheme, namely the average packet delay, throughput and end-to-end packet delay. Again, we discuss the probability-based methodology and the DTMC-based methodology in this section and in Section V, respectively. Before we present our analysis, we first define the above-mentioned performance metrics.

Firstly, the average number of TSs (or T_ps) employed until a packet is successfully transmitted is referred to as the average packet delay T_D. All the free as well as busy TSs commencing from the time the CR system is activated are included in the average packet delay quantified in terms of the number of TSs per packet [31], [32].

Secondly, the time delay between the initial attempt to transmit a packet and the final successful attempt is referred to as the packet's end-to-end packet delay [32]. We derive expressions for both the end-to-end packet delay's probability mass function as well as for the average end-to-end packet delay.

Finally, the CSR-HARQ scheme's throughput is the error-free transmission rate of the CU transmitter. Specifically, it is the total number of successfully transmitted packets per TS.

We now employ the probability-based methodology to derive the above-mentioned performance metrics.

A. AVERAGE PACKET DELAY

Encountering the corrupted packets results in retransmissions, which is the source of delay in the classical SR-HARQ scheme. However, in our proposed CSR-HARQ scheme, delay is not only due to unreliable transmissions, but also due to the unavailability of CR channels for transmission. Therefore, to analyze the packet delay of our proposed CSR-HARQ scheme, we denote the delay imposed by busy PU channels as T_{DP}. In other words, after a free TS, there is an average delay of T_{DP} while obtaining the next free TS, where $T_{DP}(i)$ is the delay, when transmissions occur in TS i after encountering $(i-1)$ busy TSs, i.e. we have $T_{DP}(i) = (i-1)T$. Following an approach similar to our previous study in [31] and [32], the average delay T_{DP} required for finding a free TS is mathematically expressed as

$$\begin{aligned} T_{DP} &= E\left[T_{DP}(i)\right] = E\left[(i-1)T\right] \\ &= \sum_{i=1}^{\infty}(i-1)TP_{on}^{i-1}(1-P_{on}) \\ &= \frac{P_{on}T}{1-P_{on}}, \end{aligned} \tag{3}$$

where P_{on} is the probability that the PU has occupied the channel, which is given in (2). When substituting $P_{on} = \beta/(\alpha+\beta)$ of (2) in equation (3), we get

$$T_{DP} = \frac{\beta T}{\alpha}. \tag{4}$$

In the free TSs, additional delays can only be imposed by the unreliable transmissions, where every retransmission imposes a delay of T seconds. Let $T_D(i)$ represent the delay of the scenario in which the CU transmitter activates i transmissions for ensuring the successful delivery of a packet. Here, $T_D(i)$ is the sum of delays in obtaining free TSs plus the delay imposed by the successful in transmission of the packets. On average total of T_{DP} seconds are needed for finding a free TS and T seconds are required for the actual round trip transmission in a free TS. Thus, we can state that

$$T_D(i) = i(T_{DP} + T). \tag{5}$$

Similar to the typical CSR-HARQ scheme, N packets are transmitted in every TS that is free. Hence, the average delay T_D of the packets is computed using

$$T_D = \frac{1}{N} E\left[T_D(i)\right] = \frac{1}{N} E\left[i(T_{DP} + T)\right]. \tag{6}$$

If P_e denotes the packet error probability (PEP) after RS decoding, then we have

$$\begin{aligned} T_D &= \frac{1}{N}\sum_{i=1}^{\infty} i(T_{DP}+T)P_e^{i-1}(1-P_e) \\ &= \frac{T}{N}\left(1+\frac{\beta}{\alpha}\right)\sum_{i=1}^{\infty} iP_e^{i-1}(1-P_e) \\ &= \frac{T}{N}\left(1+\frac{\beta}{\alpha}\right)\frac{1}{1-P_e} \text{ [seconds]} \\ &= \left(\frac{k+N}{N}\right)T_p\left(1+\frac{\beta}{\alpha}\right)\frac{1}{1-P_e} \text{ [seconds]}. \end{aligned} \tag{7}$$

After normalization of the average packet delay T_D using the packet duration T_p, T_D is given by

$$T_D = \left(\frac{k+N}{N}\right)\left(1+\frac{\beta}{\alpha}\right)\frac{1}{1-P_e} \quad [T_p's]. \tag{8}$$

Explicitly, Eq. (7) quantifies the average packet delay increases, due to increasing β/α, P_e and/or k.

B. END-TO-END PACKET DELAY

The time delay between the initial attempt to transmit a packet and the final successful attempt is referred to as the packet's end-to-end packet delay [32]. In this section, we derive expressions for both the end-to-end packet delay's probability mass function (PMF) as well as for the average end-to-end packet delay.

1) PROBABILITY MASS FUNCTION

The end-to-end delay of a packet depends on two factors: 1) the delay imposed by retransmissions, and 2) the delay incurred because of busy TSs. Let us represent the number of retransmissions of a packet by G, while the total number of busy TSs between the first transmission and the final successful reception of the packet by B. According to the principles of SR-HARQ, a retransmission does not result in the subsequently transmitted packets being discarded by the receiver, which is in contrast to the CGBN-HARQ [34]. Hence, in CSR-HARQ every retransmission results in a delay of only one T_p duration. Thus, the total end-to-end delay m suffered by a packet in units of T_p may be expressed as follows,

$$m = (G + (k+N)B + 1) \quad [T_p's], \tag{9}$$

where the final T_p interval denotes the time taken by the final successful transmission. In order to derive the end-to-end packet delay's PMF, we consider the following two scenarios.

Scenario 1: In this scenario, we assume that successful transmission is achieved in the first attempt, i.e. we have $G = 0$ and $B = 0$, which results in an end-to-end delay of $m = 1T_p$. It can be readily shown that this event has the probability of

$$P(1) = 1 - P_e. \tag{10}$$

Scenario 2: In this scenario, we assume that a successful transmission is achieved after retransmissions associated with $G \geq 1$ and $B \geq 0$ busy TSs. Below we formulate $P(m)$ for this scenario in detail.

(a) Firstly, the probability of the event that a packet is successfully transmitted after G retransmissions and B busy TS can be expressed as

$$P(G,B) = \binom{B+G-1}{B} P_{on}^B P_{off}^G P_e^G (1-P_e). \tag{11}$$

More explicitly, Eq. (11) is valid, since for the above-mentioned event the packet considered is transmitted a total of $(G+1)$ times, where the first transmission is always a failed attempt, while the final transmission is always a successful one. The B busy TSs can be any of the TSs spanning from the second to the last but one. For example, let us assume having $B = 2$ and $G = 3$. Let us assume furthermore that f, b and s denote an erroneous transmission, a busy TS and a successful transmission, respectively. Then, we have the combinations of $\{(f,f,f,b,b,s), (f,f,b,b,f,s), (f,b,b,f,f,s), (f,b,f,f,b,s), (f,b,f,b,f,s), (f,f,b,f,b,s)\}$. In other words, there are $\binom{B+G-1}{B} = \binom{4}{2} = 6$ possible ways of encountering this scenario. Hence we have:

$$P(3,2) = 6P_{on}^2 P_{off}^3 P_e^3 (1-P_e). \tag{12}$$

(b) Secondly, when we observe Eq. (9), the same delay m may be generated by multiple combinations of B and G. In this case, an exhaustive search for all possible combinations of B and G can be invoked. However, given $G \geq 1$, it can be shown that $0 \leq B \leq \left\lfloor \frac{m-2}{N+k} \right\rfloor$.

Furthermore, for a given value of B, we infer from Eq. (9) that $G = m - (k+N)B - 1$. Consequently, the probability of an end-to-end delay of m T_ps for $m > 1$ may be formulated as

$$P(m) = \sum_{B=0}^{\left\lfloor \frac{m-2}{N+k} \right\rfloor} \left(\binom{B+G-1}{B} P_{on}^{B} P_{off}^{(m-(k+N)B-1)} \cdot \cdot P_{e}^{(m-(k+N)B-1)}(1-P_e) \right), \quad m = 2, 3, \ldots \tag{13}$$

2) AVERAGE END-TO-END PACKET DELAY

The average end-to-end packet delay formula can be derived using the PMF of the end-to-end packet delay, which is given in Eqs. (10) and (13), yielding:

$$\tau = \sum_{m=1}^{M_T} m \times P_{MF}(m), \quad [T_p's] \tag{14}$$

where M_T is the maximum delay considered, which can be made sufficiently high to render the un-considered components negligible. As an example, an M_T value that satisfies $\sum_{m=1}^{M_T} P_{MF}(m) = 1 - 10^{-8}$ may be chosen.

C. THROUGHPUT

The throughput of the CR system relying on the CSR-HARQ protocol may be derived using the average delay of (7), yielding:

$$R_s = \frac{1}{T_D} \tag{15}$$

$$= \frac{N}{T} \left(\frac{\alpha}{\alpha+\beta} \right) (1-P_e) \ \text{[PPS]} \tag{16}$$

$$= \left(\frac{\alpha}{\alpha+\beta} \right) (1-P_e) \ \text{[PPTS]} \tag{17}$$

$$= \frac{N}{k+N} \left(\frac{\alpha}{\alpha+\beta} \right) (1-P_e) \ \text{[PPT}_p\text{]}. \tag{18}$$

where PPS, PPTS and PPT_p denote packet per second, packet per TS and packet per T_p, respectively. Furthermore, since we assume that an TS (N_D, K_d) code is employed, if b is the number of bits in each code word, then the throughput in units of bits per second is as follows

$$R_s = \frac{1}{T_D} \times K_d \times b \ \text{(bits per seconds)}. \tag{19}$$

Having studied the proposed CSR-HARQ scheme's performance using a probability-based methodology, in the forth coming section we will analyze the CSR-HARQ scheme using a Markov-chain-based approach.

V. MARKOV CHAIN-BASED ANALYSIS OF THE CSR-HARQ SCHEME

As in CGBN-HARQ scheme studied in [34], the performance of the CSR-HARQ can also be analysed with the aid of DTMC modelling of the state transitions. The states in the CSR-HARQ can be defined jointly by considering whether the PU channel is 'ON' or 'OFF', and by taking into account whether the packets stored in the transmitter's buffer are new packets or old packets requiring re-transmission. Note that the buffer is observed, when each TS ends. The list of states can be expressed as

$$\mathbb{S} = \{S_0, S_1, \ldots S_i, \ldots, S_{S_T}\} \tag{20}$$

where $S_T = 2^{N+1} - 1$ denotes the total number of states, while S_i represents the ith state, which is a $(N+1)$-length base-2 digit, expressed as

$$S_i = S_{i0}, S_{i1}, \ldots, S_{iN}, \quad i = 0, 1, \ldots S_T. \tag{21}$$

In Eq. (21), S_{i0} is defined as

$$S_{i0} = \begin{cases} 0, & \text{if the PU channel is free in the considered TS,} \\ 1, & \text{if the PU channel is busy in the considered TS.} \end{cases} \tag{22}$$

while S_{ij}, $j = 1, \ldots, N$, is defined as

$$S_{ij} = \begin{cases} 0, & \text{if the } j\text{th packet in state } S_i \text{ is new} \\ 1, & \text{if the } j\text{th packet in state } S_i \text{ is a retransmitted one.} \end{cases} \tag{23}$$

Based on Eqs. (22) and (23), the index of state S_i can be obtained as

$$i = \sum_{j=0}^{N} S_{ij} 2^{N-j}. \tag{24}$$

According to the above definitions, we can see that a state represents a unique combination of new or/and old packets in a free or busy TS. For showing this, below we highlight the principles of modelling with the aid of two examples. Firstly, let us consider a CSR-HARQ transmitter that transmits/retransmits a single packet in a free TS having the sensing duration of one T_p, i.e. $N = 1$ and $k = 1$. In this system, according to our definitions, the states are

$$\mathbb{S} = \{S_0, S_1, S_2, S_3\}, \tag{25}$$

where $S_0 = 00$, $S_1 = 01$, $S_2 = 10$ and $S_3 = 11$. Specifically, the first digit in a state denotes the status of the TS, while the second digit denotes the status of the packet in the transmitter buffer, as illustrated in Table 1. Given the states as shown in Eq. (25), we now proceed to find state transitions, which are demonstrated in Fig. 9. In detail, the transitions can be illustrated in Table 2. It is worth mentioning that the transition rate of states is the same as the rate of TSs.

Let us now consider the second example of modelling the CSR-HARQ scheme with the aid of the parameters $k = 1$ and $N = 4$, for the observations of 4 TSs, as shown in Fig. 10. Observe from Fig. 10 that the first TS is found to be free and 4 new packets are transmitted. Hence, the state of the transmitter in this TS is $S_0 = 00000$. However, the packet at position $e = 3$ transmitted in TS T_1 is received in error, while the following TS T_2 is found to be free. Therefore, in

TABLE 1. Possible number of states for the CSR-HARQ with $N = 1$ and $k = 1$.

Status of the TS	Status of packet	State
0 (free)	0 (new)	S_0
0 (free)	1 (old)	S_1
1 (busy)	0 (new)	S_2
1 (busy	1 (old)	S_3

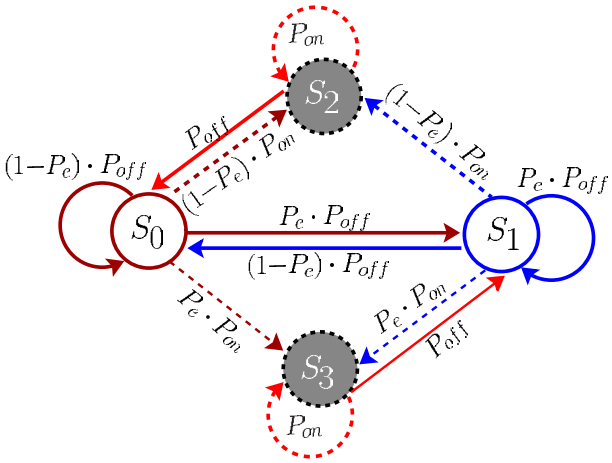

FIGURE 9. The state transition diagram for the DTMC, modelling the proposed CSR-HARQ scheme where $N = 1$ and $k = 1$. The *dashed* lines correspond to the transition towards a busy state, because the next TS is found to be a busy TS; the *solid* lines illustrate transition towards a free state due to the detection of a free TS.

TS T_2, the transmitter transmits packets 5, 6, 3 and 7, which includes the new packets 5, 6, 7 and the old packet 3, yielding a state $S_2 = 00010$. As a result, the probability of traversing from S_0 to S_2 is $P_{0,2} = P_{off}(1-P_e)^3P_e$. As shown in Fig. 10, TS T_3 is busy. Furthermore, it is observed that the two packets at positions $e = 3$ and 4, i.e., packets 3 and 7, are received in error. Hence, we have the state $S_{19} = 10011$ for TS T_3 and the probability of traversing from S_2 to S_{19} is $P_{2,19} = P_{on}(1-P_e)^2P_e^2$. Note that in the cases when two or more subsequent TSs are found busy, the transmitter's state remains the same in conjunction with the transition probability of P_{on} until a free TS is detected. Once a free TS is detected, the packets stored in the transmitter buffer are transmitted and the transmitter moves to the corresponding free state, as shown in Fig. 11. In this example, we can readily see that the state of T_4 is $S_3 = 00011$, and the probability of traversing from S_{19} to S_3 is $P_{19,3} = P_{off}$. The state transition probabilities can be found in a similar manner.

Following the above definition of states, we proceed to derive the transition probability matrix $\mathbf{P}$, where, the state transition probabilities are recorded. Assuming that at TS n, the CU transmitter is in state S_i, while at TS $n+1$, it is in state S_j, the transition probability is denoted by $P_{i,j}$. Then, according to the properties of the DTMC, this probability is independent of how the transmitter arrived at the state S_i [71], [75], which may be formulated as

$$\begin{aligned} P_{i,j} &= P\left\{S(n+1)=S_j \mid S(n)=S_i, \ldots S(1)=S_0\right\}, \\ &= P\{S(n+1)=S_j|S(n)=S_i\}, \quad \text{where} \\ 0 \le i \le S_T\ 0 \le j \le S_T &\text{ and } n = 1, 2, \ldots \end{aligned} \tag{26}$$

Furthermore, we have the properties of [71], [75]

$$\begin{aligned} 0 \le P_{i,j} \le 1. \\ \sum_{j=0}^{S_T} P_{i,j} = 1, \quad \forall\, S_i \in \mathbb{S}. \end{aligned} \tag{27}$$

For the example shown in Fig. 9, which has the states of $\mathbb{S} = S_0, S_1, S_2, S_3$, the state transition matrix $\mathbf{P}$ can be readily expressed as:

$$\boldsymbol{P} = \begin{array}{c} \\ S_0 \\ S_1 \\ S_2 \\ S_3 \end{array} \begin{array}{c} \begin{array}{cccc} S_0 & S_1 & S_2 & S_3 \end{array} \\ \begin{bmatrix} (1-P_e)P_{off} & P_eP_{off} & (1-P_e)P_{on} & P_eP_{on} \\ (1-P_e)P_{off} & P_eP_{off} & (1-P_e)P_{on} & P_eP_{on} \\ P_{off} & 0 & P_{on} & 0 \\ 0 & P_{off} & 0 & P_{on} \end{bmatrix} \end{array}.$$

The probabilities of the transmitter being in its legitimate states in TS n is $\boldsymbol{p}(n)=[P_0(n), P_1(n), \ldots, P_{S_T}(n)]^T$. Furthermore, let us assume that the transmitter commences its transmission in state $S(1) = S_0$ with the probability of $\boldsymbol{p}(1) = [1, 0, \ldots, 0, \ldots]^T$. Then, it can be shown that [71], [76]

$$\boldsymbol{p}(n+1) = \mathbf{P}^T\boldsymbol{p}(n), \tag{28}$$

$$= (\mathbf{P}^T)^n\boldsymbol{p}(1). \tag{29}$$

For our CSR-HARQ, the state transition probability matrix $\mathbf{P}^T$ is a left stochastic matrix, because the sum of each column is 1, which is shown in Eq. (27). Moreover, according to the *Perron-Frobenius theorem*, the limit of the transition matrix i.e, $\lim_{n\to\infty}(\mathbf{P}^T)^n$ exists, [76]. Hence, the Markov chain reaches its steady, when $n \to \infty$, [71], which yields

$$\boldsymbol{p}(n+1) = \boldsymbol{p}(n). \tag{30}$$

The steady-state probabilities are denoted by $\boldsymbol{\pi}$, where we have $\boldsymbol{\pi} = [\pi_0, \pi_2 \ldots, \pi_i \ldots]^T$, and the steady state probability of the transmitter being in state S_i is π_i. Then, from Eq. (30) we have

$$\boldsymbol{\pi} = \mathbf{P}^T\boldsymbol{\pi}. \tag{31}$$

Thus, the right eigenvector of $\mathbf{P}^T$ for an eigenvalue of 1 gives the steady state probabilities of all the states [71], [75], [76]. It is worth stating that the steady state probabilities fulfill the following condition

$$\sum_{j\in\mathbb{S}} \pi_j = 1 \text{ or } \boldsymbol{\pi}^T \times \mathbf{1} = 1, \tag{32}$$

where $\mathbf{1}$ is a unit column vector.

TABLE 2. Illustrates the state to state transition with respect to the event that take place.

State transition	Conditions for the event	Transition probability
$S_0 \rightarrow S_0$	Two or more error-free transmission in free TSs	$P_{00} = (1 - P_e)P_{off}$
$S_0 \rightarrow S_1$	Erroneous transmission and next TS is free	$P_{01} = P_e P_{off}$
$S_0 \rightarrow S_2$	Error-free transmission but next TS is busy	$P_{02} = (1 - P_e)P_{on}$
$S_0 \rightarrow S_3$	Erroneous transmission but next TS is busy	$P_{03} = P_e P_{on}$
$S_1 \rightarrow S_1$	Two or more erroneous transmission in free TSs	$P_{11} = P_e P_{off}$
⋮	⋮	⋮
$S_2 \rightarrow S_0$	If current TS is busy followed by a free TS given that previous transmission was error-free	$P_{20} = P_{off}$
$S_2 \rightarrow S_2$	If two or more busy TSs given that previous transmission was error-free.	$P_{22} = P_{on}$
⋮	⋮	⋮

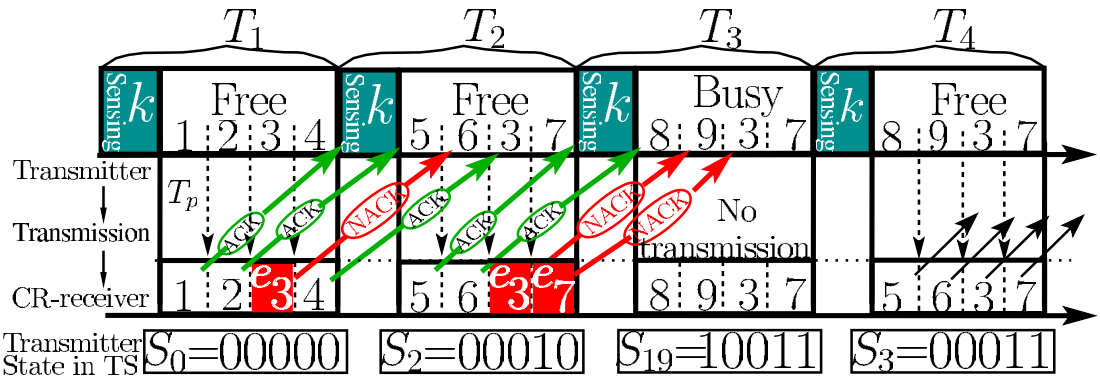

FIGURE 10. Transmission flow of CSR-HARQ in the presence of both free and busy TSs for $N = 4T_p$ and $T_s = k = 1T_p$, where the state of the transmitter is observed at the end of TSs.

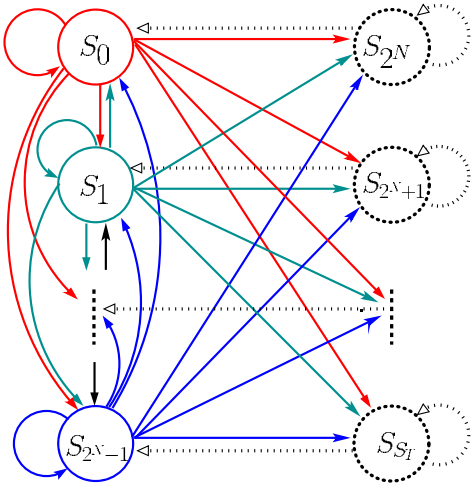

FIGURE 11. A state transition diagram for the operations of the CSR-HARQ scheme. The *solid* and *dashed* lines represent the transitions from free and busy states, respectively.

A. THROUGHPUT ANALYSIS OF CSR-HARQ SCHEME

When the DTMC reaches its steady state, the throughput of the CSR-HARQ scheme can be evaluated from the states having new packets to transmit. Hence, let $n_p(S_i)$ be the number of new packets transmitted in state S_i for $i < 2^N$, where $n_p(S_i)$ equals the number of zeros in the state sequence of S_i, excluding the first zero indicating that the TS is free. Then, the achievable throughput of the CSR-HARQ scheme can be evaluated from:

$$R_s = \sum_{i=0}^{2^N-1} \pi_i \cdot n_p(S_i), \text{ where } S_i \in \mathbb{S} \text{ [packets / TS]}. \quad (33)$$

Additionally, when expressing the throughput in terms of the number of packets per T_p, upon using $T = (N + k)T_p$, we arrive at:

$$R'_s = \frac{1}{k+N} \times R_s \quad \text{[packets / } T_p\text{]}. \quad (34)$$

Let us now study the delay performance of the CSR-HARQ scheme using the DTMC framework.

B. DELAY ANALYSIS OF CSR-HARQ

In this subsection, the average packet delay as well as the end-to-end packet delay are studied by evaluating both its probability distribution as well as the average end-to-end packet delay.

1) AVERAGE PACKET DELAY (T_D)

The average number of TSs or T_ps required for successfully delivering a packet to the receiver is the average packet delay which can be computed from the achievable throughput in Eqs. (33) and (34) as follows

$$T_D = \frac{1}{R_s} \quad \text{[TS per packet]} \tag{35}$$

$$= \frac{k+N}{R_s} \quad [T_p \text{ per packet}]. \tag{36}$$

2) END-TO-END PACKET DELAY

We continue by studying the PMF of the end-to-end packet delay. Let $\mathbb{S}_N$ be the subset of $\mathbb{S}$ defined as,

$$\mathbb{S}_N = \{S_i \mid L_i \geq 1 \text{ new packets are transmitted in } S_i\}. \tag{37}$$

In other words, $\mathbb{S}_N$ is the set of states S_i, each of which transmits one or more new packets. For each $S_i \in \mathbb{S}_N$, we define a set $\mathbb{S}_i^{(m)}$, which contains all the states S_j, where $l_{i,j} \geq 1$ new packets transmitted for the first time in state S_i are correctly received in state S_j, with exactly the delay of mT_p. This is expressed as

$$\mathbb{S}_i^{(m)} = \{S_j | l_{i,j} \geq 1 \text{ new packets transmitted in } S_i \text{ are correctly received in } S_j \text{ with a delay of } mT_p\}. \tag{38}$$

Using these definitions, the PMF of the end-to-end packet delay may be expressed as

$$P(m) = \frac{1}{c} \sum_{S_i \in \mathbb{S}_N} \sum_{S_j \in \mathbb{S}_i^{(m)}} \frac{\pi_i \times l_{i,j} \times P_{i,j}^{(m)}}{L_i}, \tag{39}$$

where $c = \sum_{S_i \in \mathbb{S}_N} \pi_i$, $P_{i,j}^{(m)}$ refers to the probability of transition from state S_i to state S_j after a delay of mT_p and $m = 1, 2, \ldots$.

The PMF of end-to-end packet delay is

$$\boldsymbol{P}_{MF} = [P(1), P(2), \ldots, P(M_T)]^T, \tag{40}$$

where M_T is the longest delay that is considered in the analysis, because the probabilities of longer delays are negligible. From the properties of the DTMC, we know that from a given state S_i, after q transitions, we have

$$\boldsymbol{p}^{(q)} = \mathbf{P}^T . \boldsymbol{p}^{(q-1)} = \cdots = (\mathbf{P}^T)^q \boldsymbol{e}_i, \quad q = 1, 2, \ldots \tag{41}$$

where $\boldsymbol{e}_i$ is the ith column of the identity matrix. From (41) it is observed that if we multiply $\mathbf{P}^T$ by the current $\boldsymbol{p}^q$, we get the following information:

a) The end-to-end delays of the packets that were transmitted for the first time in state S_i;
b) The probabilities of traversing from state S_i to any of the states in $\mathbb{S}$;
c) The number of packets $l_{i,j}$ that were transmitted for the first time in state S_i and correctly received in state S_j.

Based on the above, the state transition probability matrix $\boldsymbol{P}_{MF}$ can be updated using the following relationship

$$P(m) \leftarrow P(m) + \frac{\pi_i \times l_{i,j} \times P_{i,j}^{(m)}}{L_i}, \quad \text{where } m = 1, 2 \ldots, M_T,\ S_j \in S_i^{(m)},\ S_i \in \mathbb{S}_N. \tag{42}$$

Finally, when $\boldsymbol{P}_{MF}$ does not change, we arrive at the average end-to-end packet delay, which can be formulated as

$$\tau = \sum_{i=1}^{M_T} i \times P(i) \text{ in units of } [T_p's]. \tag{43}$$

We now validate the accuracy of the analytical results obtained through both methodologies presented in Sections IV and V using the results of our simulation-based study.

VI. PERFORMANCE RESULTS

In this section, we present the performance results of the proposed CSR-HARQ systems. The three previously stated performance metrics, namely 1) throughput 2) average packet delay, and 3) end-to-end packet delay are investigated. These metrics are evaluated in terms of the packet error probability (P_e), channel busy probability (P_{on}), the number of packets transmitted in a TS (N) and the duration k of sensing time.

In our simulations, we considered N_t TSs, which are observed and used by the CU transmitter for the successful transmission of N_s packets to the CU receiver. Note that the N_t TSs include both busy and free TSs. Hence, the throughput obtained in our simulations is evaluated as,

$$R_S' = \frac{N_s}{N_t} \times \frac{1}{k+N} \quad \text{[packets per } T_p\text{]}, \tag{44}$$

where $N_t(k+N)$ is the total number of T_ps used for transmitting N_s packets.

The throughput of the proposed CSR-HARQ is presented in Fig. 12 and 13, versus the pairwise (PEP) both for different P_{on} probability (Fig. 12) and for different values of N (Fig. 13). As seen in Fig. 12, for a given P_{on}, the throughput of the CSR-HARQ reaches its maximum when $P_e = 0$. As P_e increases, the number of retransmissions increases, hence, resulting in a reduced throughput. Furthermore, for a given P_e, Fig. 12 shows that the throughput of the CSR-HARQ is maximum, when the channel is always free from PU, i.e. when we have $P_{on} = 0$. However, when P_{on} increases, the achievable throughput of the CSR-HARQ drops significantly, since that the CU has to wait for longer to acquire free channels to send its information. In Fig. 12, we also investigate the impact of the sensing time $T_s = kT_p$ on the throughput of the CSR-HARQ. It is observed that for the cases considered when the sensing duration increases from $k = 1$ to 2, the throughput of the system reduces. Note that in Fig. 12, the throughput at $P_e = 0$ is given by

$$P_{off} \times \frac{T_d}{T} = P_{off}\left(\frac{N}{N+k}\right) = P_{off}\left(1 - \frac{k}{N+k}\right) \quad [T_p's]. \tag{45}$$

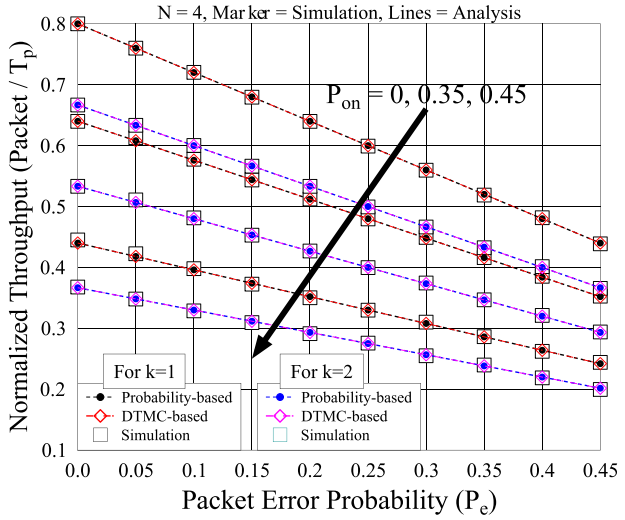

FIGURE 12. Throughput of the CSR-HARQ scheme versus packet error probability in terms of various channel busy probabilities, when $k = 1$ or 2, and $N = 4$.

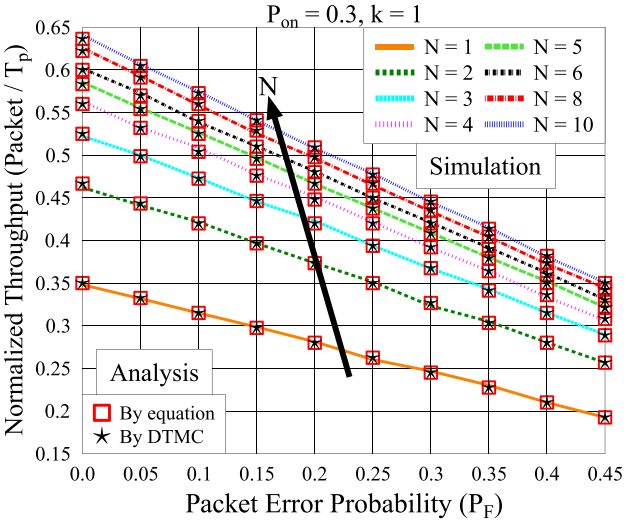

FIGURE 13. Throughput of the CSR-HARQ scheme versus packet error probability for various values of N, when $k = 1$ and $P_{on} = 0.3$.

Based on (45) we can find in Fig. 12 that for $P_e = 0$, $P_{on} = 0$ and $N = 4T_p$, the throughput is reduced from 80% to 66.67%, when the sensing duration increases from $1T_p$ to $2T_p$.

Fig. 13 shows the effect of the P_e, and the number of packets transmitted per TS on the performance of CSR-HARQ systems. It can be observed from Fig. 13 that the throughput of CSR-HARQ increases, as the value of N increases. However, when N is relatively large, such $N \geq 6$, any further increase of N only results in a marginal additional improvement of the throughput. More explicitly, this improvement remains marginal because the percentage of transmission duration, i.e. $\frac{T_d}{T} \times 100$, changes very slow, when N is relatively large. In other words, the sensing overhead per packet decreases as N increases. Furthermore, we can observe from Fig. 12 and 13 similar trends for the results obtained from the two types of analytical approaches and the simulation results, which validate the theoretical analysis.

Having characterized the throughput, let us now quantify the delay of the CSR-HARQ. Firstly, we consider the average packet delay. Again, the total time spanning from the start of PU channel sensing to the successful transmission of all the packets is taken into account. Specifically, let us assume that N_s packets are successfully transmitted within N_t TSs. Then, in our simulations, the average packet delay is characterized by

$$T_{DS} = \frac{N_t(k+N)}{N_s} \quad [T_p's]. \tag{46}$$

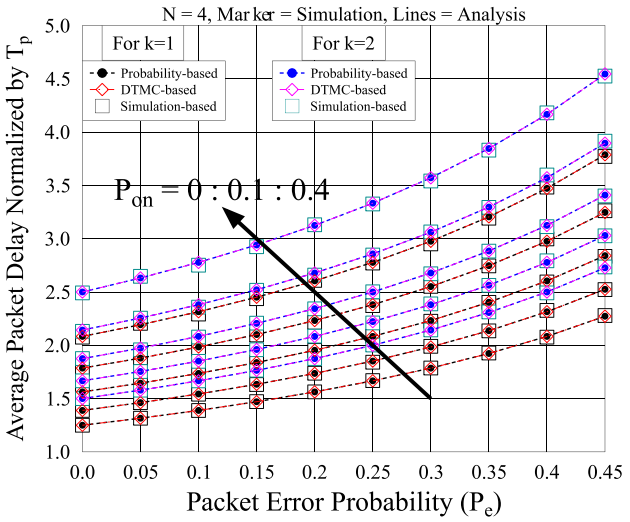

FIGURE 14. Average packet delay of the CSR-HARQ scheme versus the packet error probability (P_e) with respect to different channel busy probabilities (P_{on}), when $N = 4$ and $k = 1$ or 2.

Fig. 14 portrays the effect of P_e and P_{on} on the average packet delay. It can be observed from Fig. 14 that the average packet delay achieves its minimum, when P_e and P_{on} are zero. It increases with the increase of P_e and/or P_{on}. The reason behind this phenomenon may be explained as follows. When P_e increases, the channel becomes less reliable, which increases the number of retransmission, hence resulting in an increased delay. On the other hand, when P_{on} increases, implying that the CR system becomes busier and there are fewer opportunities for the CR system to transmit, and hence resulting in an increase of the average packet delay. Furthermore, as seen in Fig. 14, the average packet delay increases with the sensing time.

In Fig. 15, we continue to illustrate the impact of N on the average packet delay of CSR-HARQ. Explicitly, as the value of N increases, the average packet delay decreases. However, once N has reached a certain value, further increasing N does not result in any significant reduction of the average packet delay. Additionally, our theoretical results agree well with the simulation results.

Finally, we consider the end-to-end delay of the CSR-HARQ, which is evaluated in our simulations

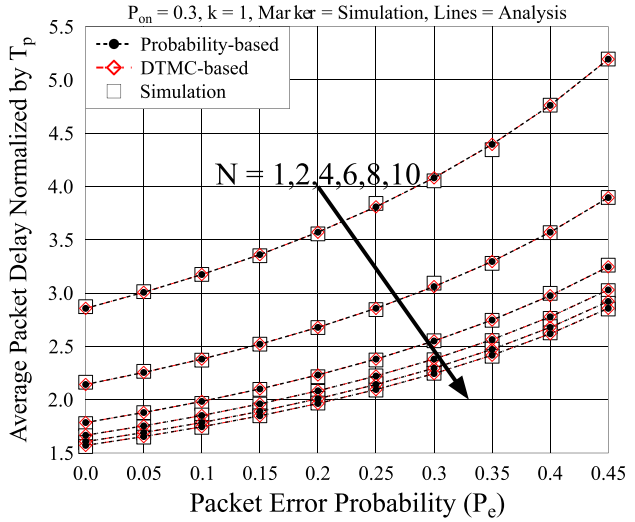

FIGURE 15. Average packet delay of the CSR-HARQ scheme with respect to different values of N, when $P_{on} = 0.3$ and $k = 1$.

as follows. Let a vector $\boldsymbol{d}$ of length N_s be used to store the delays experienced by each of the N_s packets, where $\boldsymbol{d}(j)$ is the end-to-end delay of the jth packet. Then, the PMF of the end-to-end packet delay is evaluated as [32], [34]

$$\boldsymbol{P}_d(i) = \frac{\sum_{j=1}^{N_s} \delta\left(d(j) - i\right)}{N_s}, \quad 1 \le i \le \max(\boldsymbol{d}), \qquad (47)$$

where $\max(\boldsymbol{d})$ denotes the maximum delay of the N_s packets.

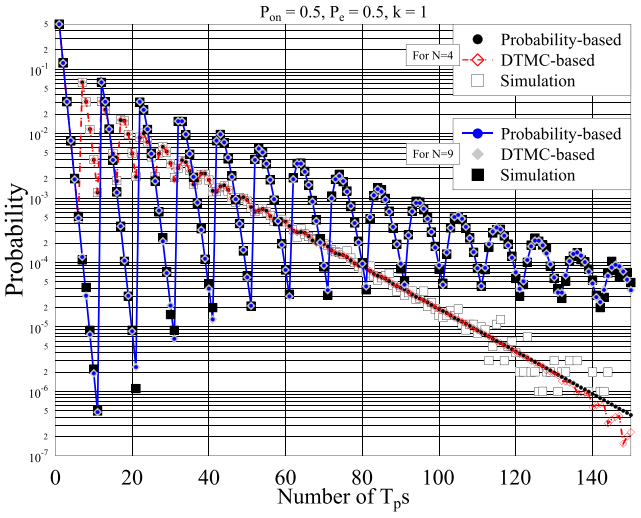

FIGURE 16. Probability of end-to-end packet delay of the CSR-HARQ systems, when $P_{on} = 0.5$, $P_e = 0.5$, $k = 1$ and $N = 4$, and 9.

Fig. 16 portrays the probability distribution obtained from our analytical approaches and simulations, when $N = 4$ and $N = 9$. It can be observed from Fig. 16 that for both cases, 50% of the packets can be correctly received in their first transmission attempt corresponding to a delay of one T_p, 12.5% of the packets are successfully received with an end-to-end delay of $2T_p$s, 3.13% packets are successfully received with an end-to-end delay of $3T_p$s, and so on. For clarity, in Fig. 16, we have used logarithmic vertical axis for plotting the PMF values.

The variations in Fig. 16 illustrate the effect of busy TSs on the end-to-end delay. For the case of $N = 4$, we can see that 6.2% of the packets are successfully received with a delay of $7T_p$, which includes the scenario of 7 transmissions of a packet without encountering busy TSs, and the scenario of 2 transmissions imposed by a busy TS. By contrast, for the case of $N = 9$, 6.2% of the packets are successfully received with a delay of $12T_p$, which includes the delay due to 12 transmissions when there is no busy TSs, as well as the delay due to one busy TS associated with 2 transmissions. Specifically, the 2 transmissions include an erroneous transmission and a successful transmission.

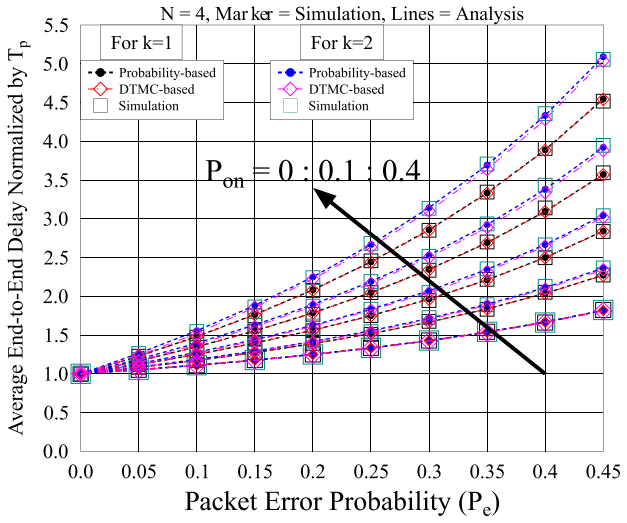

FIGURE 17. Average end-to-end packet delay of the CSR-HARQ scheme for different values of channel busy probability (P_{on}), when $N = 4$ and $k = 1$ or 2.

In Figs. 17 and 18, we demonstrate the average end-to-end packet delay, which is evaluated by the formula of

$$\tau_s = \sum_{i=1}^{\max(\boldsymbol{d})} \boldsymbol{P}_d(i) \times i \quad [T_p\text{'s}], \qquad (48)$$

in our simulations. As in Fig. 14, the average end-to-end packet delay of the CSR-HARQ is investigated for various values of P_e and P_{on}, while assuming constant values of k and N. It is found in Fig. 17 that when $P_e = 0$, the average end-to-end delay is minimum, regardless of the values of P_{on}. However, when $P_e > 0$, the average end-to-end packet delay increases with P_{on}. Furthermore, for a given value of P_{on}, the average end-to-end packet delay increases, as P_e increases.

When comparing the results of Fig. 14 and Fig. 17, we can observe the difference between the average end-to-end packet delay and the average packet delay. Firstly, it can be observed that for a given set of parameters the average end-to-end packet delay is lower than the average packet delay at $P_e = 0$. The reason behind this is that the average packet delay

TABLE 3. Performance results summary of the CSR-HARQ scheme, where results shown are normalized in unit of T_p. (a) For $P_e = 0$. (b) For $P_e = 0.2$. (c) For $P_e = 0.4$.

(a) For $P_e = 0$

P_{on}	N	R_s	T_D	τ
0	1	0.5	2	1
	3	0.75	1.33	1
	5	0.83	1.2	1
	7	0.88	1.14	1
	9	0.9	1.11	1
	10	0.91	1.1	1
0.2	1	0.4	2.5	1
	3	0.6	1	1
	5	0.67	1.5	1
	7	0.7	1.43	1
	9	0.72	1.39	1
	10	0.73	1.38	1
0.4	1	0.3	3.3	1
	3	0.45	2.22	1
	5	0.5	2	1
	7	0.53	1.9	1
	9	0.54	1.86	1
	10	0.55	1.83	1

(b) For $P_e = 0.2$

P_{on}	N	R_s	T_D	τ
0	1	0.4	2.5	1.25
	3	0.6	1.67	1.25
	5	0.67	1.5	1.25
	7	0.7	1.43	1.25
	9	0.72	1.39	1.25
	10	0.73	1.38	1.25
0.2	1	0.32	3.13	1.35
	3	0.48	2.1	1.5
	5	0.149	1.9	1.52
	7	0.56	1.8	1.8
	9	0.57	1.74	1.9
	10	0.58	1.72	1.94
0.4	1	0.24	4.2	1.6
	3	0.36	2.8	1.9
	5	0.4	2.5	2.3
	7	0.42	2.4	2.6
	9	0.43	2.31	3
	10	0.44	2.3	3.1

(c) For $P_e = 0.4$

P_{on}	N	R_s	T_D	τ
0	1	0.3	3.3	1.67
	3	0.45	2.2	1.67
	5	0.5	2	1.67
	7	0.53	1.9	1.67
	9	0.54	1.85	1.67
	10	0.55	1.83	1.67
0.2	1	0.24	4.16	2
	3	0.36	2.8	2.3
	5	0.4	2.5	2.7
	7	0.42	2.4	3
	9	0.43	2.31	3.3
	10	0.44	2.3	3.5
0.4	1	0.18	5.6	2.6
	3	0.27	3.7	3.4
	5	0.3	3.3	4.3
	7	0.31	3.2	5.2
	9	0.32	3.1	6.1
	10	0.33	3	6.6

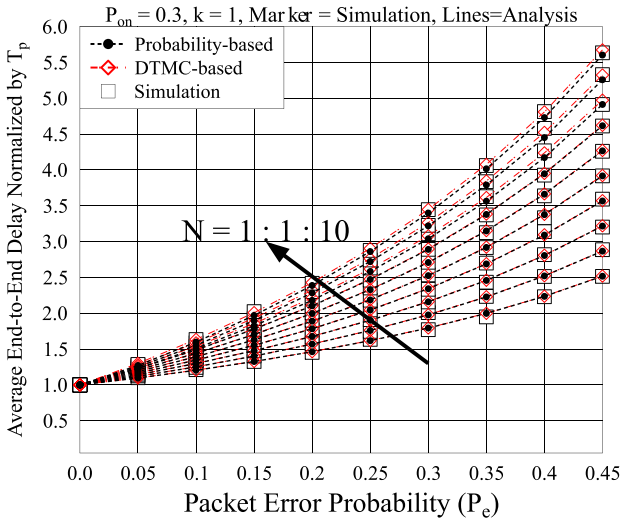

FIGURE 18. Average end-to-end packet delay of the CSR-HARQ scheme as function of packet error probability (P_e) for various values of (N), when $P_{on} = 0.3$ and $k = 1$.

includes the sensing time, the transmission time as well as the busy TSs both before and after the transmission of a packet. By contrast, the average end-to-end delay only considers the delay after the transmission of a packet. Secondly, we can find from Fig. 14 and 17 that for higher values of P_e and/or P_{on}, the average end-to-end packet delay becomes higher than the average packet delay. This is because, the average packet delay is the average transmission time of many packets, whereas, the end-to-end packet delay is the average delay per individual packet. Thirdly, when the sensing duration is increased from $k = 1$ to $k = 2$, the average end-to-end packet delay observed for a given P_e and a given P_{on} increases.

Finally, Fig. 18 shows the effect of N on the average end-to-end packet delay. Explicitly, at a given P_e, the average end-to-end packet delay increases as N increases. This is the result of the contribution made by the busy TSs to the end-to-end packet delay. Hence, for a given P_{on}, a higher N results in a longer end-to-end packet delay due to having longer busy TSs. This is in contrast to the trend depicted in Fig 15 for the average packet delay. Since, a longer TS can transmit more packets, once a free TS is acquired, the average packet delay decreases, when N increases.

VII. CONCLUSIONS

A novel CSR-HARQ transmission scheme has been proposed for a CR system to improve the exploitation of free PU channels. The proposed scheme allows a CU transmitter to sense and exploit a PU channel for its own data transmission using a modified SR-HARQ protocol. Specifically, during a TS, the CU first senses the PU channel. Once a free TS is sensed, N data packets are transmitted over the free TS. In this paper we analyzed both the throughput and delay using two analytical approaches: 1) the probability-based approach and 2) the DTMC-based approach. The performance of the proposed CSR-HARQ scheme was investigated in terms of its throughput, average packet delay and end-to-end packet delay with aid of the both closed form expressions and simulations. It can be shown that our simulation results verify the results obtained from the evaluation of our analytical formulas. Furthermore, the performance results demonstrate that both the throughput and delay of the CSR-HARQ scheme

is significantly affected both by the activity of the PU and by the channel's reliability. The throughput drops significantly, when the PU channel has a higher probability of being busy and/or when the channel's reliability becomes lower. The effect of the number of packets (N) per TS was also investigated, which shows that for higher N, the average packet delay is lower, while the end-to-end packet delay is higher. The summarized results of the CSR-HARQ are presented in the Table 3. In our future studies, we aim for evaluating the impact of the buffer resequencing technique employed at the receiver. Moreover, we intend to incorporate the effect of unreliable feedback into our future studies.

REFERENCES

[1] *Spectrum Policy Task Force Report Technical Report*, document ET Docket 02-155, FCC, Nov. 2002.
[2] G. Staple and K. Werbach, "The end of spectrum scarcity [spectrum allocation and utilization]," *IEEE Spectr.*, vol. 41, no. 3, pp. 48–52, Mar. 2004.
[3] M. A. McHenry, P. A. Tenhula, D. McCloskey, D. A. Roberson, and C. S. Hood, "Chicago spectrum occupancy measurements & analysis and a long-term studies proposal," in *Proc. 1st Int. Workshop Technol. Policy Access. Spectr. (TAPAS)*, 2006, Art. no. 1.
[4] J. Yang, "Spatial channel characterization for cognitive radios," Dept. EECS, Univ. California Berkeley, Berkeley, CA, USA, Tech. Rep. UCB/ERL M05/8, Jan. 2005. [Online]. Available: http://www.eecs.berkeley.edu/Pubs/TechRpts/2005/4293.html
[5] D. B. Cabric, "Cognitive radios: System design perspective," Ph.D. dissertation, Dept. Eng.-Elect. Eng. Comput. Sci., Univ. California Berkeley, Berkeley, CA, USA, 2007.
[6] M. H. Islam *et al.*, "Spectrum survey in Singapore: Occupancy measurements and analyses," in *Proc. 3rd Int. Conf. Cognit. Radio Oriented Wireless Netw. Commun. (CrownCom)*, May 2008, pp. 1–7.
[7] *Notice of Proposed Rulemaking, in the Matter of Unlicensed Operation in the TV Broadcast Bands and Order (ET Docket No 04-186) and Additional Spectrum for Unlicensed Devices Below 900 MHz and in the 3 GHz Band (ET Docket No. 02-380)*, document FCC 04-113, May 2004.
[8] Q. Zhao and B. M. Sadler, "A survey of dynamic spectrum access," *IEEE Signal Process. Mag.*, vol. 24, no. 3, pp. 79–89, May 2007.
[9] *Second Report and Order*, document ET docket 08-260, Washington, DC, USA, Nov. 2008.
[10] E. Hossain, D. Niyato, and Z. Han, *Dynamic Spectrum Access and Management in Cognitive Radio Networks*. Cambridge, U.K.: Cambridge Univ. Press, 2009.
[11] J. Mitola and G. Q. Maguire, Jr., "Cognitive radio: Making software radios more personal," *IEEE Pers. Commun.*, vol. 6, no. 4, pp. 13–18, Apr. 1999.
[12] S. Haykin, "Cognitive radio: Brain-empowered wireless communications," *IEEE J. Sel. Areas Commun.*, vol. 23, no. 2, pp. 201–220, Feb. 2005.
[13] M. Sherman, A. N. Mody, R. Martinez, C. Rodriguez, and R. Reddy, "IEEE Standards supporting cognitive radio and networks, dynamic spectrum access, and coexistence," *IEEE Commun. Mag.*, vol. 46, no. 7, pp. 72–79, Jul. 2008.
[14] *IEEE 802.22 Working Group on Wireless Regional Area Networks Enabling Broadband Wireless Access Using Cognitive Radio Technology and Spectrum Sharing in White Spaces*, IEEE Standard 802.22-2005, 2005.
[15] T. Fujii and Y. Suzuki, "Ad-hoc cognitive radio—Development to frequency sharing system by using multi-hop network," in *Proc. 1st IEEE Int. Symp. New Frontiers Dyn. Spectr. Access Netw. (DySPAN)*, Nov. 2005, pp. 589–592.
[16] P. Mähönen, M. Petrova, J. Riihijärvi, and M. Wellens, "Cognitive wireless networks: Your network just became a teenager," in *Proc. IEEE INFOCOM*, Apr. 2006, pp. 1–3.
[17] T. Weingart, D. C. Sicker, and D. Grunwald, "A statistical method for reconfiguration of cognitive radios," *IEEE Wireless Commun.*, vol. 14, no. 4, pp. 34–40, Aug. 2007.
[18] H. Kushwaha, Y. Xing, R. Chandramouli, and H. Heffes, "Reliable multimedia transmission over cognitive radio networks using fountain codes," *Proc. IEEE*, vol. 96, no. 1, pp. 155–165, Jan. 2008.
[19] S. Y. Jeon and D. H. Cho, "An ARQ mechanism considering resource and traffic priorities in cognitive radio systems," *IEEE Commun. Lett.*, vol. 13, no. 7, pp. 504–506, Jul. 2009.
[20] Y. Qi, R. Hoshyar, M. A. Imran, and R. Tafazolli, "H^2-ARQ-relaying: Spectrum and energy efficiency perspectives," *IEEE J. Sel. Areas Commun.*, vol. 29, no. 8, pp. 1547–1558, Sep. 2011.
[21] J. Liu, W. Chen, Z. Cao, and Y. J. Zhang, "Delay optimal scheduling for cognitive radios with cooperative beamforming: A structured matrix-geometric method," *IEEE Trans. Mobile Comput.*, vol. 11, no. 8, pp. 1412–1423, Aug. 2012.
[22] L. Musavian and T. Le-Ngoc, "Cross-layer design for cognitive radios with joint AMC and ARQ under delay QoS constraint," in *Proc. 8th Int. Wireless Commun. Mobile Comput. Conf. (IWCMC)*, Aug. 2012, pp. 419–424.
[23] W. C. Ao and K. C. Chen, "Error control for local broadcasting in heterogeneous wireless ad hoc networks," *IEEE Trans. Commun.*, vol. 61, no. 4, pp. 1510–1519, Apr. 2013.
[24] J. Hu, L. L. Yang, and L. Hanzo, "Maximum average service rate and optimal queue scheduling of delay-constrained hybrid cognitive radio in Nakagami fading channels," *IEEE Trans. Veh. Technol.*, vol. 62, no. 5, pp. 2220–2229, Jun. 2013.
[25] G. Ozcan, M. C. Gursoy, and S. Gezici, "Error rate analysis of cognitive radio transmissions with imperfect channel sensing," *IEEE Trans. Wireless Commun.*, vol. 13, no. 3, pp. 1642–1655, Mar. 2014.
[26] Y. Zou, J. Zhu, L. Yang, Y.-C. Liang, and Y.-D. Yao, "Securing physical-layer communications for cognitive radio networks," *IEEE Commun. Mag.*, vol. 53, no. 9, pp. 48–54, Sep. 2015.
[27] A. Patel, Z. Khan, S. Merchant, U. Desai, and L. Hanzo, "The achievable rate of interweave cognitive radio in the face of sensing errors," *IEEE Access*, to be published.
[28] A. Patel, M. Z. A. Khan, S. N. Merchant, U. B. Desai, and L. Hanzo, "Achievable rates of underlay-based cognitive radio operating under rate limitation," *IEEE Trans. Veh. Technol.*, vol. 65, no. 9, pp. 7149–7159, Sep. 2016.
[29] I. F. Akyildiz, W.-Y. Lee, M. C. Vuran, and S. Mohanty, "Next generation/dynamic spectrum access/cognitive radio wireless networks: A survey," *Comput. Netw. J.*, vol. 50, no. 13, pp. 2127–2159, Sep. 2006.
[30] Y. Xiao and F. Hu, *Cognitive Radio Networks*. New York, NY, USA: Auerbach, Jan. 2009.
[31] A. U. Rehman, L.-L. Yang, and L. Hanzo, "Performance of cognitive hybrid automatic repeat request: Stop-and-wait," in *Proc. IEEE 81st Veh. Technol. Conf. (VTC Spring)*, May 2015, pp. 1–5.
[32] A. U. Rehman, C. Dong, L.-L. Yang, and L. Hanzo, "Performance of cognitive stop-and-wait hybrid automatic repeat reQuest in the face of imperfect sensing," *IEEE Access*, vol. 4, pp. 5489–5508, Jul. 2016.
[33] A. U. Rehman, L. L. Yang, and L. Hanzo, "Performance of cognitive hybrid automatic repeat reQuest: Go-Back-N," in *Proc. IEEE 83rd Veh. Technol. Conf. (VTC Spring)*, May 2016, pp. 1–5.
[34] A. U. Rehman, C. Dong, V. A. Thomas, L.-L. Yang, and L. Hanzo, "Performance of cognitive hybrid automatic repeat reQuest: Go-Back-N," *IEEE Access*, Nov. 2016.
[35] J. Lai, E. Dutkiewicz, R. P. Liu, and R. Vesilo, "Opportunistic spectrum access with two channel sensing in cognitive radio networks," *IEEE Trans. Mobile Comput.*, vol. 14, no. 1, pp. 126–138, Jan. 2015.
[36] G. Ozcan and M. Gursoy, "Throughput of cognitive radio systems with finite blocklength codes," *IEEE J. Sel. Areas Commun.*, vol. 31, no. 11, pp. 2541–2554, Nov. 2013.
[37] S. Stotas and A. Nallanathan, "Enhancing the capacity of spectrum sharing cognitive radio networks," *IEEE Trans. Veh. Technol.*, vol. 60, no. 8, pp. 3768–3779, Oct. 2011.
[38] I. F. Akyildiz, W.-Y. Lee, M. C. Vuran, and S. Mohanty, "A survey on spectrum management in cognitive radio networks," *IEEE Commun. Mag.*, vol. 46, no. 4, pp. 40–48, Apr. 2008.
[39] T. Yucek and H. Arslan, "A survey of spectrum sensing algorithms for cognitive radio applications," *IEEE Commun. Surveys Tuts.*, vol. 11, no. 1, pp. 116–130, 1st Quart., 2009.
[40] E. Axell, G. Leus, E. G. Larsson, and H. V. Poor, "Spectrum sensing for cognitive radio: State-of-the-art and recent advances," *IEEE Signal Process. Mag.*, vol. 29, no. 3, pp. 101–116, May 2012.
[41] Y.-C. Liang, Y. Zeng, E. C. Y. Peh, and A. T. Hoang, "Sensing-throughput tradeoff for cognitive radio networks," *IEEE Trans. Wireless Commun.*, vol. 7, no. 4, pp. 1326–1337, Apr. 2008.

[42] W. Tang, M. Z. Shakir, M. A. Imran, R. Tafazolli, and M. S. Alouini, "Throughput analysis for cognitive radio networks with multiple primary users and imperfect spectrum sensing," *IET Commun.*, vol. 6, no. 17, pp. 2787–2795, Nov. 2012.

[43] W. Liang, S. X. Ng, J. Feng, and L. Hanzo, "Pragmatic distributed algorithm for spectral access in cooperative cognitive radio networks," *IEEE Trans. Commun.*, vol. 62, no. 4, pp. 1188–1200, Apr. 2014.

[44] Y.-C. Liang, K.-C. Chen, G. Y. Li, and P. Mahonen, "Cognitive radio networking and communications: An overview," *IEEE Trans. Veh. Technol.*, vol. 60, no. 7, pp. 3386–3407, Sep. 2011.

[45] C. Cormio and K. R. Chowdhury, "A survey on MAC protocols for cognitive radio networks," *Ad Hoc Netw.*, vol. 7, no. 7, pp. 1315–1329, Sep. 2009.

[46] A. De Domenico, E. C. Strinati, and M.-G. Di Benedetto, "A survey on MAC strategies for cognitive radio networks," *IEEE Commun. Surveys Tuts.*, vol. 14, no. 1, pp. 21–44, 1st Quart., 2012.

[47] S. Lin and D. J. Costello, *Error Control Coding: Fundamentals and Applications*, 2nd ed. Upper Saddle River, NJ, USA: Prentice-Hall, 1999.

[48] L. Hanzo, T. Liew, B. Yeap, R. Tee, and S. X. Ng, *Turbo Coding, Turbo Equalisation and Space-Time Coding: EXIT-Chart-Aided Near-Capacity Designs for Wireless Channels*. New York, NY, USA: Wiley, 2011.

[49] G. Yue, X. Wang, and M. Madihian, "Design of anti-jamming coding for cognitive radio," in *Proc. IEEE Global Telecommun. Conf.*, Nov. 2007, pp. 4190–4194.

[50] G. Yue and X. Wang, "Design of efficient ARQ schemes with anti-jamming coding for cognitive radios," in *Proc. IEEE Wireless Commun. Netw. Conf. (WCNC)*, Apr. 2009, pp. 1–6.

[51] Y. Liu, Z. Feng, and P. Zhang, "A novel ARQ scheme based on network coding theory in cognitive radio networks," in *Proc. IEEE Int. Conf. Wireless Inf. Technol. Syst. (ICWITS)*, Aug. 2010, pp. 1–4.

[52] R. Zhang and L. Hanzo, "Superposition-aided delay-constrained hybrid automatic repeat reQuest," *IEEE Trans. Veh. Technol.*, vol. 59, no. 4, pp. 2109–2115, May 2010.

[53] R. Zhang and L. Hanzo, "A unified treatment of superposition coding aided communications: Theory and practice," *IEEE Commun. Surveys Tuts.*, vol. 13, no. 3, pp. 503–520, 3rd Quart., 2011.

[54] B. Makki, A. G. I. Amat, and T. Eriksson, "HARQ feedback in spectrum sharing networks," *IEEE Commun. Lett.*, vol. 16, no. 9, pp. 1337–1340, Sep. 2012.

[55] B. Makki, T. Svensson, and M. Zorzi, "Finite block-length analysis of spectrum sharing networks using rate adaptation," *IEEE Trans. Commun.*, vol. 63, no. 8, pp. 2823–2835, Aug. 2015.

[56] H. A. Ngo and L. Hanzo, "Hybrid automatic-repeat-reQuest systems for cooperative wireless communications," *IEEE Commun. Surveys Tuts.*, vol. 16, no. 1, pp. 25–45, 1st Quart., 2014.

[57] W. Liang, H. V. Nguyen, S. X. Ng, and L. Hanzo, "Adaptive-TTCM-aided near-instantaneously adaptive dynamic network coding for cooperative cognitive radio networks," *IEEE Trans. Veh. Technol.*, vol. 65, no. 3, pp. 1314–1325, Mar. 2016.

[58] J. G. Kim and M. M. Krunz, "Delay analysis of selective repeat ARQ for a Markovian source over a wireless channel," *IEEE Trans. Veh. Technol.*, vol. 49, no. 5, pp. 1968–1981, Sep. 2000.

[59] K. Ausavapattanakun and A. Nosratinia, "Analysis of selective-repeat ARQ via matrix signal-flow graphs," *IEEE Trans. Commun.*, vol. 55, no. 1, pp. 198–204, Jan. 2007.

[60] L. Badia, M. Levorato, and M. Zorzi, "Markov analysis of selective repeat type II hybrid ARQ using block codes," *IEEE Trans. Commun.*, vol. 56, no. 9, pp. 1434–1441, Sep. 2008.

[61] L. Badia, "A markov analysis of selective repeat ARQ with variable round trip time," *IEEE Commun. Lett.*, vol. 17, no. 11, pp. 2184–2187, Nov. 2013.

[62] H. Chen, R. G. Maunder, and L. Hanzo, "A survey and tutorial on low-complexity turbo coding techniques and a holistic hybrid ARQ design example," *IEEE Commun. Surveys Tuts.*, vol. 15, no. 4, pp. 1546–1566, 2013.

[63] B. Zhang, H. Chen, M. El-Hajjar, R. Maunder, and L. Hanzo, "Distributed multiple-component turbo codes for cooperative hybrid ARQ," *IEEE Signal Process. Lett.*, vol. 20, no. 6, pp. 599–602, Jun. 2013.

[64] F. Chiti, R. Fantacci, and A. Tassi, "Evaluation of the resequencing delay for selective repeat ARQ in TDD-based wireless communication systems," *IEEE Trans. Veh. Technol.*, vol. 63, no. 5, pp. 2450–2455, Jun. 2014.

[65] C. Dong, L.-L. Yang, J. Zuo, S. X. Ng, and L. Hanzo, "Energy, delay, and outage analysis of a buffer-aided three-node network relying on opportunistic routing," *IEEE Trans. Commun.*, vol. 63, no. 3, pp. 667–682, Mar. 2015.

[66] C. Dong, L. L. Yang, and L. Hanzo, "Performance of buffer-aided adaptive modulation in multihop communications," *IEEE Trans. Commun.*, vol. 63, no. 10, pp. 3537–3552, Oct. 2015.

[67] W.-C. Ao and K.-C. Chen, "End-to-end HARQ in cognitive radio networks," in *Proc. IEEE Wireless Commun. Netw. Conf. (WCNC)*, Apr. 2010, pp. 1–6.

[68] S. Touati, H. Boujemaa, and N. Abed, "Cooperative ARQ protocols for underlay cognitive radio networks," in *Proc. 21st Eur. Signal Process. Conf. (EUSIPCO)*, Sep. 2013, pp. 1–5.

[69] E.-Y. Park, M.-G. Song, W. Choi, and G.-H. Im, "Maximization of long-term average throughput for cooperative secondary system with HARQ-based primary system in cognitive radio network," *IEEE Commun. Lett.*, vol. 20, no. 2, pp. 356–359, Feb. 2016.

[70] R. A. Roshid, N. M. Aripin, N. Fisal, S. H. S. Ariffin, and S. K. S. Yusof, "Integration of cooperative sensing and transmission," *IEEE Veh. Technol. Mag.*, vol. 5, no. 3, pp. 46–53, Sep. 2010.

[71] D. Bertsekas and R. Gallagher, *Data Networks*, 2nd ed. Englewood Cliffs, NJ, USA: Prentice-Hall, 1991.

[72] R. Fantacci, "Queuing analysis of the selective repeat automatic repeat reQuest protocol wireless packet networks," *IEEE Trans. Veh. Technol.*, vol. 45, no. 2, pp. 258–264, May 1996.

[73] L. Badia, M. Rossi, and M. Zorzi, "SR ARQ packet delay statistics on Markov channels in the presence of variable arrival rate," *IEEE Trans. Wireless Commun.*, vol. 5, no. 7, pp. 1639–1644, Jul. 2006.

[74] A. Leon-Garcia and I. Widjaja, *Communication Networks*. New York, NY, USA: McGraw-Hill, 2004.

[75] R. Howard, *Dynamic Probabilistic Systems: Markov Models*. New York, NY, USA: Wiley, 1971.

[76] R. A. Horn and C. R. Johnson, *Matrix Analysis*. Cambridge, U.K.: Cambridge Univ. Press, 2012.

ATEEQ UR REHMAN received the B.Eng. degree in computer science and information technology from the Islamic University of Technology, Dhaka, Bangladesh, in 2009. He is currently pursuing the Ph.D. degree in wireless communications with the University of Southampton, under the supervision of Prof L.-L. Yang and Prof L. Hanzo. He then joined Abdul Wali Khan University Mardan, Pakistan, as a Lecturer with the Department of Computer Science. His main research interests are next generation wireless communications and cognitive radio networks, particularly cross layer approach and Hybrid ARQ.

VARGHESE ANTONY THOMAS received the B.E. (Hons.) degree in electrical and electronics engineering from the Birla Institute of Technology and Science, Pilani, in 2010, the M.Sc. degree in wireless communications from the University of Southampton, U.K., in 2011, and the Ph.D. degree from the University of Southampton in 2015. He was in wireless communications research Group with the University of Southampton. He is currently a Research Associate with the Georgia Institute of Technology, USA. His research interests are mainly in optical communications, optical-wireless integration, backhaul for MIMO, and radio over fiber systems. He is a recipient of the several academic awards including the Commonwealth Scholarship of the Government of U.K. and the Mayflower Scholarship of the University of Southampton.

LIE-LIANG YANG (M'98–SM'02–F'16) received the B.Eng. degree in communications engineering from Shanghai TieDao University, Shanghai, China, in 1988, and the M.Eng. and Ph.D. degrees in communications and electronics from Beijing Jiaotong University, Beijing, China, in 1991 and 1997, respectively. In 1997, he was a Visiting Scientist with the Institute of Radio Engineering and Electronics, Academy of Sciences of the Czech Republic. Since 1997, he has been with the University of Southampton, U.K., where he is currently the Professor of Wireless Communications with the School of Electronics and Computer Science. He has authored over 300 research papers in journals and conference proceedings. He has authored or co-authored three books and also published several book chapters. His research has covered a wide range of topics in wireless communications, networking, and signal processing. He is a fellow of the IET. He has served as an Associate Editor of the IEEE Transactions on Vehicular Technology and the Journal of Communications and Networks, and is currently an Associate Editor of the IEEE Access and the *Security and Communication Networks Journal*.

LAJOS HANZO (F'04) received the master's degree in electronics in 1976 and the Ph.D. degree in 1983, and the D.Sc degree. Since 1986, he has been with the School of Electronics and Computer Science, University of Southampton, U.K. He has successfully supervised 110 Ph.D. students, co-authored 20 John Wiley/IEEE Press books on mobile radio communications totalling in excess of 10 000 pages, published 1600+ research entries at the IEEE Xplore, acted both as a TPC and the General Chair of IEEE conferences, presented keynote lectures and has been awarded a number of distinctions. He is currently directing a 60-strong academic research team, where he is involved on a range of research projects in the field of wireless multimedia communications sponsored by industry, the Engineering and Physical Sciences Research Council U.K., the European IST Program, and the Mobile Virtual Center of Excellence, U.K. He is a FREng, FIET, fellow of EURASIP. In 2009, he was awarded the honorary doctorate Doctor Honoris Causa by the Technical University of Budapest and in 2015 by the University of Edinburgh. During his 40-year career in telecommunications he has held various research and academic posts in Hungary, Germany, and the U.K. He holds the Chair in telecommunications with the University of Southampton.. He is an enthusiastic Supporter of Industrial andAcademic Liaison and he offers a range of industrial courses. He is also a Governor of the IEEE VTS and of COMSOC. From 2008 to 2012, he was the Editor in-Chief of the IEEE Press and a Chaired Professor with Tsinghua University, Beijing. His research is Funded by the European Research Council's Senior Research Fellow Grant.